
REVIEW AND COMPARISON OF MHD WAVE CHARACTERISTICS AT THE SUN AND IN EARTH'S MAGNETOSPHERE

M.A. Chelpanov

*Institute of Solar-Terrestrial Physics SB RAS,
Irkutsk, Russia, max_chel@iszf.irk.ru*

S.A. Anfinogentov

*Institute of Solar-Terrestrial Physics SB RAS,
Irkutsk, Russia, anfinogentov@iszf.irk*

D.V. Kostarev

*Institute of Solar-Terrestrial Physics SB RAS,
Irkutsk, Russia, kostarev@iszf.irk.ru
Geophysical Centre RAS,
Moscow, Russia*

O.S. Mikhailova

*Institute of Solar-Terrestrial Physics SB RAS,
Irkutsk, Russia, o_mikhailova@iszf.irk.ru*

A.V. Rubtsov

*Institute of Solar-Terrestrial Physics SB RAS,
Irkutsk, Russia, avrubtsov@iszf.irk.ru*

V.V. Fedenev

*Institute of Solar-Terrestrial Physics SB RAS,
Irkutsk, Russia, fedenev@iszf.irk.ru*

A.A. Chelpanov

*Institute of Solar-Terrestrial Physics SB RAS,
Irkutsk, Russia, chelpanov@iszf.irk.ru*

Abstract. Magnetohydrodynamic (MHD) waves play a crucial role in the plasma processes of stellar atmospheres and planetary magnetospheres. Wave phenomena in both media are known to have similarities and unique traits typical of each system.

MHD waves and related phenomena in magnetospheric and solar physics are studied largely independently of each other, despite the similarity in properties of these media and the common physical foundations of wave generation and propagation. A unified approach to studying MHD waves in the Sun and Earth's magnetosphere opens up prospects for further progress in these two fields.

The review examines the current state of research into MHD waves in the Sun's atmosphere and Earth's magnetosphere. It outlines the main features of the wave propagation media: their structure, scales, and typical parameters. We describe the main theoretical models

applied to wave behavior studies; discuss their advantages and limitations; compare characteristics of MHD waves in the Sun's atmosphere and Earth's magnetosphere; and review observation methods and tools to obtain information on waves in various media.

Keywords: magnetohydrodynamics, MHD waves, Alfvén waves, fast magnetosonic waves, slow magnetosonic waves, magnetosphere, ULF waves, chromosphere, solar corona, active regions, solar activity.

CONTENT

Introduction.....	4
1 Key medium parameters.....	5
1.1 Solar chromosphere.....	5
1.2 Solar corona.....	5
1.3 Earth's magnetosphere.....	6
2 Theoretical description: approaches and limits of applicability.....	7
3 Peculiarities of observations of MHD waves in different media.....	8
3.1 Slow magnetosonic waves.....	8
3.2 Fast magnetosonic waves.....	10
3.3 Alfvén waves.....	11
3.4 Wave resonators.....	13
4 Classification of waves in the magnetosphere.....	15
5 Wave observation facilities.....	15
5.1 Observing the Sun in the optical range.....	15

5.2	Observing the solar corona in the EUV range.....	16
5.3	Observing the Sun in the radio range.....	16
5.4	<i>In situ</i> observations of the Sun.....	17
5.5	Satellite observations in Earth's magnetosphere.....	17
5.6	Radar observation of magnetospheric ULF waves.....	18
6	Discussion and conclusion.....	19
	References.....	20

INTRODUCTION

Most of the matter in the Universe is plasma. Despite common mechanisms of generation, propagation, and dispersion of waves in it, there are specific features related to medium parameters and magnetic field structure in various regions of outer space. The most explorable media in outer space are the Sun's atmosphere and Earth's magnetosphere. While there are significant differences in characteristic magnetic field and plasma density magnitudes, Earth's magnetosphere and solar active regions have many similar parameters. The characteristic size of solar active region is $\sim 10^5$ km and is close to the size of Earth's magnetosphere. Both in the coronal part of active region and in the magnetosphere, the Alfvén velocity is close to 1000 km/s; the similarities between their characteristic scales and velocities determine the close characteristic periods of the processes. Both in solar active regions and in Earth's magnetosphere, characteristic wave periods range from tens of seconds to tens of minutes.

Historically, the research in these two fields in different scientific communities developed almost independently, thereby producing various methods and theories for describing similar processes. At the same time, ideas about penetration of oscillations from interplanetary space into the magnetosphere began to appear in the 1970s [Troitskaya et al., 1971; Guglielmi, 1974] and later stimulated interest among many researchers [Baumjohann et al., 1984; Hasegawa, Chen, 1974; Mazur, 2010; Potapov, Mazur, 1994]. Theoretical justification for penetration of fast magnetoacoustic waves through the transition layer has been proposed in [Leonovich et al., 2003]. Satellite and radar data were used to search for the relationship between wave events in space environments [Potapov, Polyushkina, 2010; Stephenson, Walker, 2002]. Kepko and Spence [2003] have revealed that the periodic fluctuations in the solar wind pressure correspond to electromagnetic pulsations in the magnetosphere. The authors suggested that the source of the latter may be forced magnetosonic oscillations transmitted from the solar wind. The oscillations generated outside the magnetosphere include those whose spectra are similar to the spectra of oscillations in the solar wind. For instance, Kepko et al. [2002] note that the characteristic frequency set common to waves in the magnetosphere also dominates in the spectrum of oscillations observed in the solar wind. Potapov et al. [2013] analyze similarities between the oscillation spectra at the base of coronal holes and the oscillations of the interplanetary magnetic field (IMF) near Earth's orbit for individual observations. As an attempt to find a link

between magnetospheric pulsations and oscillations observed directly in the solar photosphere, we can mention the study into the 0.1–5 Hz ion-cyclotron waves in the polar cap in the vicinity of open field lines. They feature frequency modulation with a period ~ 5 min coinciding with the periods of 5 min oscillations recorded in the solar photosphere [Guglielmi, Dovbnaya, 1973; Guglielmi et al., 2015]. Generation of such oscillations, also known as serpentine emissions, and their relationship with oscillations of the photosphere need further study since no explanations for them have been offered yet.

Also of interest is to compare the oscillations that are observed in the Sun's atmosphere and Earth's magnetosphere. Theoretically, waves with minute periods should be described in these media by the same theory — magnetic hydrodynamics (MHD) [Zelenyi, Veselovsky, 2008]. Nevertheless, approaches to studying these waves in the vicinity of Earth and in the Sun's atmosphere differ significantly. In Earth's magnetosphere, the electromagnetic field and plasma parameters are directly measured at any point, whereas studies into solar oscillations always represent an outside perspective covering the entire solar disk or active region. However, such a difference in the possibilities of observations may eventually provide a positive cumulative effect due to the same theoretical basis of the processes under study. The possibility of using the methods developed in solar physics for analyzing magnetospheric MHD waves and, vice versa, applying the methods used in magnetospheric physics to the Sun has already been discussed and remains one of the most promising ways for researchers of these two fields to cooperate [Nakariakov et al., 2016b].

The review compares particular wave phenomena in the Sun's atmosphere and Earth's magnetosphere, examines similarities and differences between them. The emphasis is on those plasma features in which the magnetic field plays a dominant role or is similar in order of magnitude to gas pressure ($\beta < 1$, where $\beta = 8\pi P/B^2$ is the ratio of the gas-dynamic pressure to the magnetic one). In the solar atmosphere, this criterion is valid for chromospheric and higher layers. In the magnetosphere, this condition holds almost everywhere.

This review develops the ideas of combining the approaches of studying MHD waves in the solar corona and Earth's magnetosphere, suggested in [Nakariakov et al., 2016b]. We also pay attention to the methods of observing waves and to the solar chromosphere. In addition, the paper presents new results obtained after publication of [Nakariakov et al., 2016b], such as observations of standing waves in coronal loops, which allow them to be identified as slow magnetoacoustic waves

[Mandal et al., 2016], analysis of undamped kink oscillations of coronal loops [Anfinogentov et al., 2015], study into the conditions for the occurrence of instabilities [Klimushkin et al., 2017; Rubtsov et al., 2020], etc. The review is aimed at making up for the shortage in the literature in Russian on this topic. It can be useful for graduate students and experts in solar-terrestrial physics for research and work with students. It can also help in developing a new interdisciplinary field of research on waves in plasma systems.

1. KEY MEDIUM PARAMETERS

This section provides a general description and presents key parameters of the media under study, such as characteristics of particle populations, fields, structural morphological features. The description sequence has been chosen according to the direction of propagation of the main energy flux — from the lower layers of the Sun's atmosphere through the corona to the magnetosphere.

1.1. Solar chromosphere

The chromosphere is a layer of the Sun's atmosphere in which, as compared to the underlying photosphere, the temperature rises sharply to 10^4 – 10^5 K [Song et al., 2010]. In the photosphere, gas pressure plays a crucial role, whereas magnetic pressure prevails in the corona [Zhang et al., 1991]. Thus, gas and magnetic pressures in the chromosphere are comparable in magnitude, which defines it as a highly dynamic region in which there are many structural inhomogeneities such as chromospheric network, filaments, spicules [Snodgrass, Wilson, 1993; Sterling, 2000; Feldman et al., 2000]; and, in addition, sunspots and faculae in active regions (Figure 1). In the chromosphere there are many magnetoplasma loops of different heights; these loops are generally asymmetric: at one footpoint the magnetic field strength is significantly higher than at the other [Wiegmann et al., 2010].

Chromospheric magnetic fields are concentrated in thin tubes ~ 100 km thick, the field strength in which is $\sim 10^3$ G (0.1 T). Hereafter, since different units of measurement are widely used for physical quantities in magnetospheric and solar physics, both are given for improved readability [Zayer et al., 1989]. Magnetic fields in the quiet Sun's regions are associated with supergranulation, the greatest observable manifestation of convection on the Sun's surface.

Supergranulation cells have a typical size of ~ 30000 km and a lifespan up to two days [Rincon, Rieutord, 2018].

The chromospheric network has the geometry of the supergranulation cells and consists of separate small and large nodes with diameters of 1000 and 2000–8000 km respectively. Large nodes are clusters of small ones [Robustini et al., 2019]. At the boundaries of the chromospheric network's cells, spicules are formed — plasma jets, which are elongated features ejected from the Sun's surface into its atmosphere (150–200 km in diameter, ~ 10000 km in height) [De Pontieu et al., 2007b].

Chromospheric plasma consists mainly of hydrogen ions and to a lesser extent of helium. The typical number density of hydrogen ions in the chromosphere is 10^{10} cm $^{-3}$.

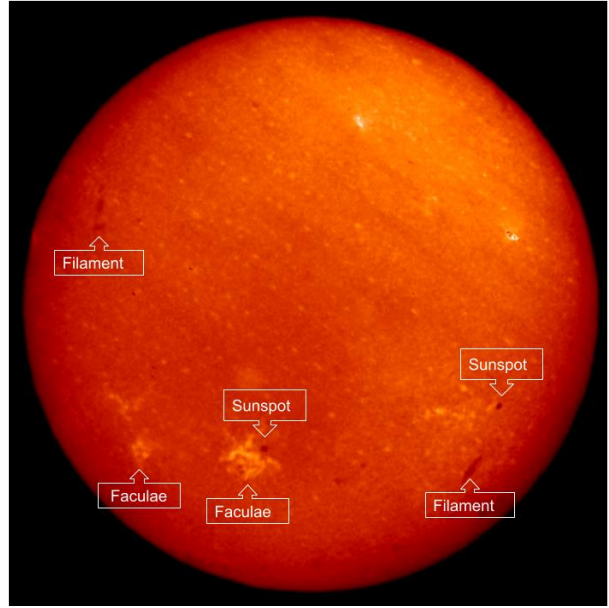


Figure 1. Solar disk image taken on October 27, 2021 by a full-disk telescope in the H α line (ISTP SB RAS Baikal Astrophysical Observatory) [Trifonov et al., 2004]. Sunspots, filaments, and faculae are shown

The strength of magnetic fields in the chromosphere varies widely: from tens to several thousands of gauss (10^{-3} – 10^{-1} T). The smallest values are observed in the chromospheric network's cells. At the cell edges, the field strength is increased due to the fact that plasma with magnetic lines frozen into it is transferred by supergranulation motions to edges of the cells, where it begins to sink, thereby producing clusters of magnetic tubes. The most concentrated fields are observed in sunspots, where the strength is as high as thousands of gauss (0.1 T).

1.2. Solar corona

The solar corona is the least dense and the hottest part of the solar atmosphere. The corona is completely filled with plasma (temperature $\sim 10^6$ K, number density $\sim 10^8$ – 10^9 cm $^{-3}$) consisting mainly of ionized hydrogen and doubly ionized helium admixed with multiply ionized atoms of heavier elements. The magnetic field in the corona varies from a few gauss ($\sim 10^{-4}$ T) in quiet regions to hundreds or even thousands of gauss ($\sim 10^{-2}$ – 10^{-1} T) [Anfinogentov et al., 2019] in active regions above large sunspots. Nonetheless, almost everywhere in the corona the magnetic pressure significantly exceeds the gas pressure ($\beta \ll 1$) and hence largely determines the evolution and structuring of coronal plasma. Owing to low β , the transfer of matter and heat across the magnetic field is suppressed, resulting in strong plasma fragmentation and field-aligned plasma inhomogeneities in the corona [van Doorselaere et al., 2008]. In the images captured in EUV emission lines, these inhomogeneities are seen as bright arcades stretched along the magnetic field (Figure 2). Such structures are called coronal loops and usually have the form of thin long loops with increased brightness in EUV lines, ~ 1000 km in thickness and hundreds of thousands of kilometers in length [Brueckner, Bartoe, 1974].

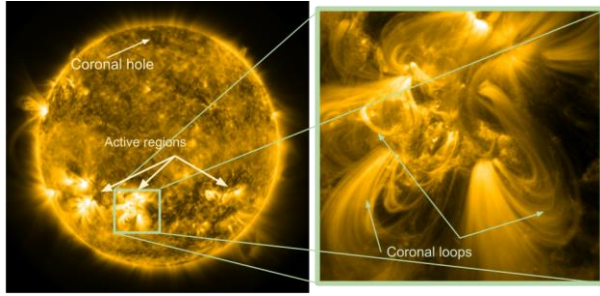


Figure 2. Full solar disk image (left) taken by the Atmospheric Imaging Assembly (AIA) on board the Solar Dynamics Observatory (SDO) in the 171 Å line. On the right is an enlarged image segment with an active region

The brightest and densest coronal loops are located above active regions and are connected with places of concentration of strong magnetic fields on the photosphere. Magnetic field lines in active regions generally emerge from the photosphere and return back to it, without reaching interplanetary space. Thus, coronal plasma in active regions is trapped in the lower solar corona and does not leak into interplanetary space. Due to the enhanced plasma density, active regions in the EUV images are seen as places of increased emission brightness. Along with the bright active regions there are extensive dark regions — coronal holes [Altschuler et al., 1972]. Magnetic fields in them generally have an open configuration, field lines in which go into interplanetary space and are stretched by the solar wind up to the boundaries of the Solar System. Coronal plasma in these regions is no longer trapped inside the lower corona, but constantly flows out into the solar wind — a supersonic plasma stream moving from the corona into the interplanetary space [Krieger et al., 1973]. As a result, plasma density in coronal holes is much lower than in active regions, and the holes themselves look like dark features in EUV images. The solar wind has a significant impact on the configuration of magnetic fields of planets, forming a bow shock on the subsolar side and creating an extended tail of field lines on the other. The characteristic values of the solar wind density in the Earth orbit are 1–10 cm⁻³ (on average ~5 cm⁻³) [Dmitriev et al., 2009]. Inhomogeneities of matter and field parameters in the solar wind due to variable effects on the magnetosphere generate regular geomagnetic disturbances.

1.3. Earth's magnetosphere

Medium parameters in Earth's magnetosphere differ significantly from those observed in the surrounding solar wind. The main differences are the magnetic field strength approximately by an order of magnitude greater and also the plasma density by an order of magnitude lower (except for the plasmasphere — a region of the magnetosphere adjacent to the ionosphere, which has a higher density of cold plasma) [Mead, Fairfield, 1975]. There are, however, a number of spatial regions inside the magnetosphere, whose characteristics differ significantly, which affects electromagnetic wave propagation in it. Boundaries of such regions can be created by resonators and waveguides, with dimensions and their other

parameters changing over time under the influence of fluctuations in the solar wind speed and density, as well as in the IMF orientation [Klimushkin, 1998]. Accordingly, the properties of electromagnetic waves propagating in them or experiencing resonant amplification, including the range of ultralow-frequency (ULF) waves (waves with a frequency lower than the proton gyrofrequency), also change [Guglielmi, Potapov, 2017]. In Earth's magnetosphere, they play a crucial role, for example, they can accelerate charged particles, creating so-called killer electrons that have a destructive effect on satellite equipment, as well as can affect the shape of auroras and motion of their arcs [Baddeley et al., 2017]. The magnetospheric regions that are specific for ULF wave propagation and generation can be called the regions exhibiting increased densities of particles involved in the resonant interaction with waves, such as the ring current forming region.

The boundary of the magnetosphere is the magnetopause. Its position is determined by the balance of pressures of the incoming solar wind particle flux and the magnetic field. It also depends on the IMF direction [Samsonov et al., 2013]. At a distance of (4–5) R_E (25–35 thousand km, where $R_E = 6371$ km is the Earth radius) from the magnetopause in the Earth—Sun direction in the solar wind there is a bow shock driven by a supersonic particle flux continuously incident on the magnetosphere. The transition region between these two surfaces (magnetosheath) is characterized by turbulent plasma motions and the absence of the large-scale ordered magnetic field structure [Vaisberg, Smirnov, 2008; Rakhmanova et al., 2021]. The plasma density and the magnetic field strength in it are higher than in the solar wind (tens of cm⁻³ and tens of nT — 10⁻⁴ G respectively), and the ion temperature is lower (of order of a few keV). At the same time, the transverse thermal velocity far exceeds the parallel one [Crooker et al., 1976]. The parameter $\beta > 1$ varies widely. The plasma stream velocity in the subsolar part of the magnetosheath decreases to a subsonic one. In the transition region, there are generally solar wind particles, but also there is a small amount of plasma of magnetospheric origin, including oxygen ions [Marcucci et al., 2004]. It penetrates there during reconnection of field lines and when crossing the magnetopause in moving along the gyroradius [Eastmann, Frank, 1982; Papamastorakis et al., 1984].

Near Earth, the magnetic field is close to the dipole one. This approximation is suitable for describing the magnetic field structure within a distance of several R_E (several tens of thousands of kilometers). Near the Earth surface in the vicinity of the magnetic equator, the magnetic field strength is $\sim 3 \cdot 10^4$ nT (0.3 G). In the outer magnetosphere, the field differs from the dipole one — it is compressed on the subsolar side, and on the opposite side it forms a tail stretched by tens of millions of kilometers away from the Sun. According to the orientation of the geomagnetic field, in the southern part (lobe) of the tail the field is directed from Earth; in the northern one, toward Earth. The magnetic field topology in the magnetosphere is defined by the solar wind incident on the magnetosphere, as well as by a number of current sys-

tems in the magnetosphere and at its boundary [Parker, 1958]. Among them are Chapman—Ferraro currents — surface currents at the magnetopause that shield the magnetospheric field; currents flowing across the magnetotail and closing through the magnetopause; ring current; field-aligned currents closing in the high-latitude ionosphere [Ganushkina et al., 2018].

Magnetospheric plasma consists mainly of protons and electrons. Its main sources are the solar wind, from which plasma enters through the magnetopause and cusps, and Earth’s ionosphere, which, inter alia, is a source of heavier ions — oxygen. The fraction of heavy ions and hence the average mass of particles increase toward Earth [Welling et al., 2015]. In the magnetosphere, a number of charged particle populations differing in composition, energy, and lifetime are identified. Moreover, their distribution depends on geomagnetic conditions [Kotova et al., 2008].

In the magnetospheric region closest to Earth — the plasmasphere — the cold plasma density is by orders of magnitude higher than in the surrounding space environment. Its shape is close to the torus bounded by the field lines at $(4\div 7)R_E$ from the center of Earth near the equator. The outer boundary of the plasmasphere features a steep gradient of plasma density and is called the plasmopause. In data from the satellites crossing it, it is visible by the change in plasma density tens of times (Figure 3). The plasma energy in the plasmasphere is of the order of and less than a few electron-volts.

The plasmopause is also a boundary of the region in which the predominant electric field is the corotation field created in a fixed coordinate system by plasma rotation in the geomagnetic field [Kotova et al., 2008]. Outside the plasmopause, the convective plasma motion from the magnetotail to Earth under the impact of the dawn-dusk electric field prevails. The inner boundary of the plasmasphere is rather arbitrary: it smoothly passes into the ionosphere. The plasmasphere is generally thought to be located at 1000 km above the Earth surface.

Particles with higher energies than in the plasmasphere make up the ring current. Under quiet conditions, it is located outside the plasmasphere and extends to $(7\div 10)R_E$ from Earth’s center. Energies of its constituent particles generally range from 10 to 200 keV. The main ions of the ring current are protons; besides them there are oxygen ions, whose number, however, is several times

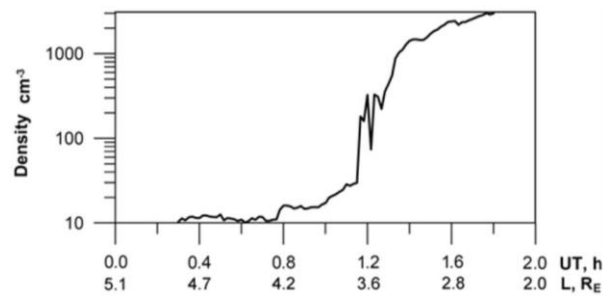


Figure 3. Proton density as recorded by the Van Allen Probes B satellite on December 25, 2014. The satellite moved to Earth and crossed the plasmopause at ~01:10 UT

smaller under quiet geomagnetic conditions, as well as inclusions of nitrogen and helium. At the same time, influenced by geomagnetic activity, densities and energies of ring current particles of different types experience significant variations [Kovtyukh, 2001]. Among characteristic features are also radiation belts — two regions acting as magnetic traps for high-energy particles. The inner belt is located within the plasmasphere and contains protons with energies of hundreds of MeV and electrons with energies of hundreds of keV. The outer belt in the radial direction has a width of several Earth radii with maximum electron density at $(4\div 5)R_E$ from Earth’s center. It is mainly filled with electrons with energies of the order of tens of MeV. A detailed overview of the structure and dynamics of the hot plasma distribution in the magnetosphere is presented in [Kovtyukh, 2001].

2. THEORETICAL DESCRIPTION: APPROACHES AND LIMITS OF APPLICABILITY

Rigorous theoretical description of plasma should be based on kinetic equations for electrons and ions. This approach takes into account the motion and the generated electromagnetic field of each individual particle, as well as the interaction between fields and particles. It is quite complex and not always rational. As shown in [Braginsky, 1963], the MHD approach can be applied to many problems. In this approach, plasma is described by a system of equations for the evolution of local macroscopic quantities such as density, pressure, temperature, magnetic field, and velocity of macroscopic flows. Adopting the MHD approach usually requires the fulfillment of a number of conditions.

1. The characteristic time of the process under study is significantly longer than the mean free time of particles in plasma, as well as than the periods of plasma oscillations and Larmor gyration of particles.
2. The mean free path and the Larmor radius are much shorter than the characteristic spatial scale of the process considered.
3. The characteristic speeds of the process of interest are much lower than the speed of light.

Obviously, these conditions are not always met, for example, in Earth’s magnetosphere, where plasma can be considered as collisionless. Nevertheless, for collisionless plasma in some cases it is possible to obtain qualitatively correct results with the aid of the MHD approach [Volkov, 1964].

The dispersion relation for MHD waves in a homogeneous plasma has the form [Leonovich, Mazur, 2016]

$$\begin{aligned} & (\omega^2 - k_{\parallel}^2 V_A^2) \times \\ & \times [\omega^4 - k^2 (V_S^2 + V_A^2) \omega^2 + k^2 k_{\parallel}^2 V_S^2 V_A^2] = 0, \end{aligned} \quad (1)$$

where ω is the wave frequency; $k = \sqrt{k_{\parallel}^2 + k_{\perp}^2}$ is the wave number (k_{\parallel} , k_{\perp} are the wave vector components directed respectively along and across magnetic field lines); V_A is the Alfvén velocity; V_S is the sound velocity.

ty. This equation has three eigensolutions:

$$\omega^2 = k_{\parallel}^2 V_A^2, \quad (2)$$

the Alfvén mode is transverse oscillations whose group velocity $v_{grA} = \frac{\partial \omega}{\partial k} = V_A \left(\frac{\vec{B}_0}{B_0} \right)$ is directed along magnetic field lines:

$$\omega^2 = \frac{1}{2} k^2 (V_S^2 + V_A^2) \pm \sqrt{\frac{1}{4} k^4 (V_S^2 + V_A^2)^2 - k^2 k_{\parallel}^2 V_S^2 V_A^2}, \quad (3)$$

where the solution with "-" before the radical describes slow mode; and that with "+", fast mode. In most real plasma features, one of the conditions usually holds: $V_S \gg V_A$, which corresponds to $\beta \gg 1$; $V_S \gg V_A (\beta \ll 1)$; $|k_{\parallel}| \ll |k_{\perp}|$. In this case, the dispersion expression for slow mode takes the form

$$\omega^2 \approx k_{\parallel}^2 V_S^2 V_A^2 / (V_S^2 + V_A^2), \quad (4)$$

and for fast mode

$$\omega^2 \approx k^2 (V_S^2 + V_A^2). \quad (5)$$

The group velocity of slow mode is directed, as in the case of Alfvén waves, along the background magnetic field, and the group velocity of fast mode is directed along the wave vector, i.e. the wave propagates isotropically relative to the background magnetic field.

The MHD equations can be derived from kinetic equations in certain approximations. In this case, the following limitations are imposed on the model:

1. The energy distribution function of particles is isotropic and equilibrium (close to the maxwellian one) [Akhiezer et al., 1974].

2. The wave phase velocity is higher than the average thermal velocity of particles, i.e. resonant processes (Landau damping [Landau, 1946]) can be neglected.

3. The frequencies of the described oscillations are significantly lower than the cyclotron and plasma frequencies of plasma particles ($\omega \ll \omega_{ci}$).

4. In the case of collisionless plasma, the magnetic pressure is higher than the gas dynamic pressure ($\beta < 1$).

It should be noted here that the second limitation automatically excludes slow modes whose phase velocity is close to the thermal velocity of particles from consideration. For Earth's magnetosphere, the MHD approach is therefore applicable only for disturbances of Alfvén or fast modes. Unlike the conditions in the Sun's atmosphere, there are practically no regions with large β ($\beta \gg 1$) in the dipole-like part of Earth's magnetosphere. To describe the the wave-particle interaction, as well as to study the magnetospheric analogues of slow magnetoacoustic waves, it is necessary to use a kinetic approach. Furthermore, additional imitations are imposed on the applicability of MHD modeling, which are associated with the configuration of the background magnetic field linked to the motion of particles of certain types (bounce motion in the magnetosphere, electric and magnetic drifts). The characteristic times of these mo-

tions may be comparable to the wave period, which should foster the wave—particle interaction. For plasma in an inhomogeneous curvilinear magnetic field (dipole-like), this means the following.

1. The wave frequency should be significantly higher than the frequency of ion oscillations between conjugate points near the ionosphere, or the bounce frequency ($\omega \gg \omega_{bi}$).

2. The wave frequency should be much higher than the bounce-period-averaged frequency of ion motion around Earth due to the drift caused by the geomagnetic field inhomogeneity and the curvature of field lines — the magnetic drift frequency ($\omega \gg \omega_{di}$) [Klimushkin et al., 2021].

With a pure MHD approach, it is impossible to account for resonant wave—particle interactions such as particle acceleration by waves, and, vice versa, energy transfer from particles to wave. Such interactions can be taken into account in hybrid approaches, where elements of kinetic theory are introduced [Borovsky, 1993], but the applicability of each of them should be considered separately.

Note that there are MHD models that allow for the presence of particles of several types in plasma. Such models are called multifluid. They were developed to describe a wide variety of wave phenomena [Khomenko, 2020], but we do not discuss them in this review.

The kinetic approach has wider limits of applicability, allowing us to describe waves in plasma with high accuracy in a wide range of parameters. For the case when the wave frequency is much lower than the gyrofrequency of ions and electrons, the kinetic approach can be simplified to gyrokinetic. This is the branch of kinetics in which particle motions are averaged over the phase of rotation around a field line of the background magnetic field [Antonsen, Lane, 1980; Catto et al., 1981].

Unlike Earth's magnetosphere, plasma of the solar corona is collisional, and the MHD approximation holds almost everywhere since the characteristic spatial scales of wave phenomena range from one to hundreds of thousands of kilometers and significantly exceed the free path of particles, as well as the Debye and Larmor radii. The characteristic periods (tens of seconds – hours) are by many orders of magnitude longer than the period of plasma oscillations and Larmor gyration.

3. PECULIARITIES OF OBSERVATIONS OF MHD WAVES IN DIFFERENT MEDIA

3.1. Slow magnetosonic waves

In the research into the Sun's atmosphere, the wave type is determined from a number of indirect characteristics: frequency, propagation velocity, type of physical structure in which oscillations are observed. The specific set of characteristics depends on the type of observation (spectral or imaging observation), the structure observed, and the layer of the solar atmosphere. It is often difficult to attribute the detected oscillations to one or another wave type because of data limitation or ambiguity in the characteristics. For example, when observing

similar oscillations simultaneously in two spectral lines formed in different layers of the solar atmosphere, we can track wave propagation between these layers. Thus, we can record wave propagation frequency and velocity if the distance between the formation heights of the spectral lines observed is known. Solar atmosphere models can provide physical parameters of medium in the height range of interest, which makes it possible to identify the type of MHD modes, using wave parameters obtained from observations.

If waves are observed in solar corona images captured in optically thin coronal lines, to identify the type of wave and its mode it is important to know the direction of propagation of the apparent wave front, its phase velocity, the oscillation period, and the character of the displacement of plasma structures. The Alfvén speed and the sound velocity in the corona differ by about an order of magnitude (~ 150 and ~ 1000 km/s), which makes it possible, with available wave phase velocity measurements, to unambiguously separate fast and slow mode waves. In the case of standing waves in coronal structures, the difference between phase velocities of fast and slow modes reflects in equally strong differences between characteristic oscillation periods. Moreover, observing the waves in images enables us not only to measure the phase velocity and the oscillation period, but also to determine the spatial configuration of wave disturbances, thereby identifying the observed oscillatory mode of plasma inhomogeneity (the main wave modes of magnetic flux tube are described in Section 3.2).

Slow modes on the Sun are observed in all atmospheric layers from the photosphere to the corona. They were among the first to be identified in the chromosphere in sunspot umbra, where their observational manifestations are known as three-minute oscillations in sunspot umbra and running penumbral waves (see the review [Bogdan, 2000]). With the advent of space tools observing the Sun in EUV, it was found that three-minute oscillations in sunspots penetrate into the corona and propagate in quasi-open funnel structures (coronal fans) connected with the sunspot in the form of traveling compression/rarefaction waves propagating at a speed of ~ 150 km/s, close to the speed of sound in the corona [De Moortel, 2009; Kobanov et al., 2013]. Along with sunspots, propagating slow modes are also observed in facular regions, as well as in their associated coronal structures (see the review [De Moortel, 2009]). In this case, the characteristic periods can be as long as 10–15 min. According to generally accepted concepts, the period of these waves is determined by gravity-related dispersion effects in the Sun’s lower atmosphere (the temperature minimum and chromosphere zone). These effects make propagation of slow modes in the Sun’s atmosphere possible only if their frequency exceeds the acoustic cutoff frequency

$$\omega_{\text{cf}} = \frac{\gamma g}{2c_s} \cos \theta, \quad (6)$$

where γ is the adiabatic index; $g \approx 274$ m/s² is free fall acceleration; c_s is the speed of sound; θ is the angle be-

tween the magnetic field vector and the vertical direction. The cutoff frequency itself is the natural oscillation frequency of the respective atmospheric layer, and any broadband impact causes oscillations with a frequency close to ω_{cf} . The period corresponding to acoustic cutoff (6) is the shortest in the temperature minimum — the layer located directly under the chromosphere. In this region, the cutoff period at $\gamma=5/3$ and $\theta=0$ is ~ 3 min. In the chromosphere, this period is equal to 5 min and is well manifested in the spectrum of oscillations observed in the chromosphere of faculae [Balthasar, 1990; De Pontieu et al., 2005]. When the magnetic field vector deviates from the vertical direction, the cut-off period increases and can be as long as 10–15 min or more. In the corona, due to the high temperature, ω_{cf} turns out to be significantly lower than photospheric values, which leads to the fact that the slow modes formed in the temperature minimum and chromosphere propagate almost without dispersion effects associated with gravitational stratification.

In addition to quasi-open coronal structures, slow modes are observed in hot coronal loops formed during flares [Ofman, Wang, 2002]. In this case, a coronal loop acts as a resonator, and its length and temperature determine the oscillation period observed. Standing and traveling slow modes in coronal structures are often called longitudinal modes in the literature, although, according to the theory of MHD waves in magnetic cylinder independently developed in [Zaitsev, Stepanov, 1975] and [Edwin, Roberts, 1983], they are slow sausage modes. Standing slow modes in coronal loops were first detected in the EUV spectrum by the Solar Ultraviolet Measurements of Emitted Radiation (SUMER) instrument and were named SUMER-oscillations [Wang et al., 2003]. The subsequent commissioning of space imaging EUV telescopes, such as TRACE and SDO/AIA, made it possible to observe these oscillations directly in the form of brightness variations along the loop and to finally confirm that they are of the nature of slow modes in the coronal loop resonator [Mandal et al., 2016]. Analysis of imaging observations of slow modes in hot loops has shown that along with classical standing waves sloshing oscillations are often observed, which are a fairly short-time broadband slow mode disturbance propagating along the loop and reflected several times from its footpoints.

In the magnetosphere, according to theoretical concepts [Yumoto, 1985; Leonovich et al., 2006], slow modes can be generated as follows: a fast mode wave penetrates into the magnetosphere and transforms into a slow mode on a resonant surface — a magnetic shell, where the resonant frequency of slow MHD waves is equal to the frequency of the passing fast wave. Slow modes feature strong dissipation, as a result of which energy and momentum are actively transmitted to background plasma particles and the wave damps very quickly [Leonovich, Mazur, 2013; 2016]. Presumably, that is why the slow mode is not observed in Earth’s magnetosphere. The drift compressional mode can be considered the closest to the slow mode in properties (low frequencies and large longitudinal magnetic field

component) [Mager et al., 2013]. It is described by one of the solutions of gyrokinetic equations and is a consequence of the finite plasma pressure and its inhomogeneity across magnetic field lines [Mikhailovskii, Fridman, 1967]. Frequencies of such waves coincide in order of magnitude with frequencies of the diamagnetic particle drift caused by plasma inhomogeneity. The drift-compressional wave is characterized by coupling with the Alfvén wave due to the curvature of magnetic field lines [Klimushkin, Mager, 2011; Klimushkin et al., 2012]. Another solution to the kinetic equations is the mirror mode, which is also compressional and is represented by the longitudinal magnetic field disturbance. Its existence requires a significant excess of the transverse thermal velocity of particles over the parallel one [Hasegawa, 1969].

3.2. Fast magnetosonic waves

In the solar atmosphere, fast magnetosonic waves are most clearly observed in the solar corona. They can arbitrarily be divided into global and local fast magnetosonic waves. The former are often driven by solar flares and coronal mass ejections and appear as compression/rarefaction waves propagating over long distances of the order of the solar radius and longer [Uchida et al., 1973; Wang, 2000]. Using SDO data, continuous transverse oscillations have been shown to occur in coronal holes in the lower corona [McIntosh et al., 2011; Thurgood et al., 2014; Weberg et al., 2018]. Local fast mode waves are observed in coronal magnetoplasma loops. Since a coronal loop is a waveguide for fast mode waves, several waveguide modes differing in their dispersion properties and observational manifestations can be formed in it. Depending on the azimuthal wave number m , sausage mode ($m=0$), kink mode ($m=1$), and ballooning¹, fluting, ($m>1$) modes are distinguished [Zaitsev, Stepanov, 1975; Edwin, Roberts, 1983; Nakariakov, Verwichte, 2005]. The last ones are rarely used for theoretical interpretation of phenomena in the solar corona since observations of these modes are hindered by the small transverse size of coronal loops.

Vibrational modes of a magnetic tube with different azimuthal wave numbers are shown in Figure 4. The sausage mode is characterized by significant perturbations of the plasma density when the cross-section of the loop expands and contracts, whereas its axis remains stationary. Due to the dispersion properties, the sausage mode is trapped inside the waveguide only at sufficiently large longitudinal wave numbers (see Equations (7)–(9) in Section 3.4), when the wavelength is commensurate with the transverse diameter of the loop. Thus, the oscillation period of the sausage mode is defined by the transverse scales of the loop; in coronal conditions, it is about 10 s. Small values of the periods make it difficult to observe the sausage mode in EUV images owing to the insufficiently high observational cadence. For this reason, observational manifestations of sausage waves are generally recorded in the radio range as quasi-periodic

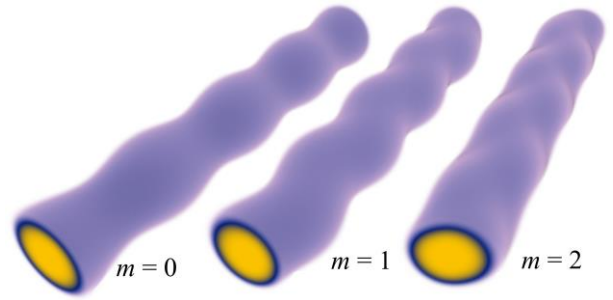


Figure 4. Oscillation modes of magnetic tube depending on the azimuthal wave number: radial ($m=0$), kink ($m=1$), and fluting ($m=2$) modes

variations in the microwave emission [Reznikova et al., 2015].

In the kink mode, the density perturbations are very weak, but the loop axis is displaced. This makes the kink mode similar in its properties to the oscillations of a guitar or a violin string. The kink mode turns out to be trapped inside a coronal loop at any values of the longitudinal wave number; therefore, the main longitudinal harmonic whose wavelength is equal to twice the length of the loop is most often observed. In this case, the oscillation period depends on the loop length and usually amounts to minutes or tens of minutes, which is much longer than the period of sausage oscillations [Nakariakov, Verwichte, 2005]. In coronal loops, the kink mode is observed in two modes: high amplitude decaying oscillations and low amplitude decayless oscillations.

High amplitude decaying oscillations are excited by an external impulsive driver, associated, e.g., with coronal mass ejection, and very quickly decay. The characteristic decay time is usually about 3–4 oscillation periods. Another mode of kink oscillations has been found relatively recently and features very small (200 km) displacements of oscillating loops and the absence of visible damping [Anfinogentov et al., 2015]. The latter, however, does not mean that dissipation does not occur. The wave is most likely constantly supplied with energy from outside, for example, according to the principle of self-oscillating process [Nakariakov et al., 2016a].

The physical mechanism responsible for the rapid damping of kink fast mode oscillations of coronal loops is still not clearly defined. The most popular theory suggests that the damping is caused by resonant absorption [Ruderman, Roberts, 2002]. Since the phase velocity of kink oscillations is higher than the Alfvén velocity inside the loop, but lower than the Alfvén velocity outside it, there is a resonant layer (magnetic shell of the loop) in the transition layer between the inner part of the loop and the background plasma, where the kink speed is equal to the local Alfvén velocity. In this layer, there is a possibility of converting fast mode waves into unobservable torsional Alfvén waves, which carry away energy from the fast mode wave, causing its damping.

In the magnetosphere, a significant part of MHD wave phenomena is excited by mechanisms operating outside the magnetosphere [Zong, 2022]. The driving force of these waves is the solar wind: shear flows on the flanks of the magnetosphere; fluctuations; waves

¹Russian names of these modes have not completely well-established yet and may seem strange. For instance, ballooning modes in this context have nothing in common with ballooning instability.

outside the magnetosphere; transient phenomena inherent in the solar wind or generated by the solar wind–magnetosphere coupling. At the boundary of the magnetosphere, the solar wind also stimulates nonstationary processes such as the Kelvin–Helmholtz instability [Mazur, Chuiko, 2017]. These processes generate a fast mode wave at the boundary of the magnetosphere, which propagates deep into the magnetosphere to a reflection surface. Thus, a fast mode resonator is formed in the transition region of the magnetosphere. It is bounded by the magnetopause on one side and by the reflection surface on the other. However, part of the fast mode energy can tunnel out of the resonator and propagate even deeper into the magnetosphere until it reaches a resonant magnetic shell, where its frequency will coincide with the Alfvén wave frequency. On this shell, the fast mode wave is transformed into an Alfvén wave due to the Alfvén resonance (Figure 5). The Alfvén resonance phenomenon was first established in the simplest model of the magnetosphere with straight field lines and an inhomogeneous magnetic field across field lines [Southwood, 1974; Chen, Hasegawa, 1974a, b]. Later it was shown that the Alfvén resonance can also exist in more complex models such as the two-dimensional inhomogeneous model of the magnetosphere, in particular in a dipole magnetic field, given the curvature of field lines and the plasma inhomogeneity along the magnetic field [Lifshits, Fedorov, 1986; Leonovich, Mazur, 1989].

Thus, fast mode waves exist both in the Sun’s atmosphere and in Earth’s magnetosphere. In both cases, the nature of the waves is determined by the resonant properties of plasma inhomogeneities. Near Earth, the magnetosphere as a whole plays the role of a resonator, whereas on the Sun such resonators are magnetoplasma loops and other structures of the solar corona. The resonant absorption of a kink fast mode wave by converting its energy into the Alfvén mode has a direct analogue in magnetospheric physics when the energy of fast mode waves penetrating into the magnetosphere from the outside is pumped into Alfvén oscillations on a resonant magnetic shell. In the magnetospheric physics, this phenomenon is known as the Alfvén resonance; in the solar physics, as the resonant absorption.

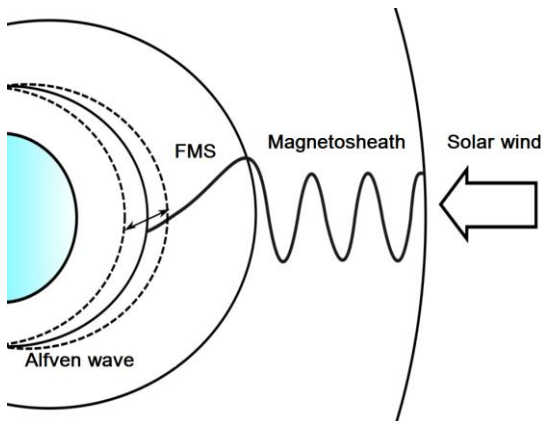


Figure 5. A scheme of excitation of Alfvén resonance by a fast mode wave tunneling into the magnetosphere by a resonator in the magnetosheath

It is noteworthy that in the solar atmosphere the fast mode part of this process is well pronounced, whereas in the magnetosphere the Alfvén waves arising during this process are regularly observed and best studied. This information from magnetospheric physics can also shed light on Alfvén waves, which can occur in coronal loops due to resonant absorption. Obviously, to obtain a detailed physical picture of the conversion of fast mode waves into Alfvén waves, it is necessary to integrate both theoretical and observational data collected for both the magnetosphere and the Sun.

3.3. Alfvén waves

In a homogeneous plasma, Alfvén waves are transverse waves in which only the magnetic field is disturbed, whereas the density, temperature, and gas dynamic pressure remain constant. The Alfvén disturbance is a transverse displacement of magnetic field lines. It propagates in the form of a wave whose group velocity is directed parallel to the magnetic field vector, and is analogous to the transverse vibrations of a stretched string. In the case of inhomogeneous structured plasma, magnetic field lines are not straight; Alfvén waves generally turn out to be coupled with other wave modes such as fast mode [Glassmeier et al., 2003]. Consequently, the assignment of specific wave modes to Alfvén modes in an inhomogeneous plasma proves to be rather arbitrary. In solar physics, it is customary to assign to Alfvén waves only such wave modes that in the linear approximation of ideal plasma do not perturb plasma density and temperature, but cause disturbances of the magnetic field and the local plasma velocity. An observational signature of the latter is the nonthermal broadening of spectral lines. As far as we know, there are no other observable manifestations of Alfvén waves in the solar corona, and there can also be other causes for the nonthermal broadening of spectral lines itself. This makes it extremely difficult to detect Alfvén waves in the corona and makes them practically invisible to existing observational instruments. On the other hand, magnetospheric physics also assign to Alfvén waves those transverse waves that exhibit density disturbances occurring due to the medium nonuniformity and the curvature of magnetic field lines. Nevertheless, these waves satisfy dispersion relation (2) for Alfvén waves. Below we examine the Alfvén waves in detail as they are understood by researchers in both the magnetosphere and the Sun.

The solar atmosphere is highly inhomogeneous at all levels from the photosphere to the corona. In the corona, the inhomogeneities are generally elongated in the direction along the field and have characteristic transverse dimensions of the order of 1 Mm, and longitudinal dimensions of the order of 100 Mm. In the first approximation, they can be described by a magnetic flux tube or magnetic cylinder model. In the framework of this model, the inhomogeneity is a spatial region bounded by a field-aligned cylindrical surface. The plasma parameters inside the magnetic flux tube are considered uniform and differ significantly from those of the background plasma. Examples of such inhomogeneities are coronal loops, filaments, as well as chromospheric spicules and fibrils. As mentioned above, in solar physics

only those wave modes are taken as Alfvén waves that do not perturb the plasma density and temperature, and all motions occur only along magnetic shells. In magnetic flux tubes, wave motions of only one type are possible which do not perturb the plasma density — torsional Alfvén oscillations. In this case, Alfvén waves propagate along the axis of the structure in the form of torsional motions of particular magnetic surfaces and hence are a direct analogue of the toroidal Alfvén wave in Earth’s magnetosphere.

Alfvén waves are one of the probable agents for energy transfer from the lower layers of the Sun’s atmosphere to the corona. In coronal holes, Alfvén waves can propagate to large heights, and, according to some views, up to interplanetary space [Marsch, 2018]. In this case, favorable conditions are determined mainly by open magnetic field lines in coronal holes [Banerjee et al., 1998]. According to one of the assumptions, Alfvén waves are excited by magnetic reconnections in the chromospheric network and contribute to turbulence of the plasma flow from coronal holes [Marsch, 2018]. Cranmer et al. [2007] and Wang [2009] have shown that Alfvén waves are generated by convective motions in the solar photosphere.

The difficulty in studying Alfvén waves on the Sun, in contrast to Earth’s magnetosphere, is that they are difficult to detect by remote observations. The reason is that Alfvén waves do not cause plasma density perturbations and hence do not affect the intensity of electromagnetic emission in the optical and ultraviolet ranges. Therefore, the reports on observations of Alfvén waves in the emission intensity [De Pontieu et al., 2007a] are probably explained by the erroneous interpretation of the kink fast mode of magnetic flux tube as the Alfvén one. Furthermore, Alfvén waves are local disturbances, i.e. wave motions on neighboring magnetic surfaces are independent and generally do not coincide in phase and frequency. As a result, Alfvén waves should not manifest themselves in the observed line-of-sight velocities measured from the Doppler shift of spectral lines, but should lead to their broadening. This defines the theoretical possibility of detecting Alfvén waves through observations of periodic nonthermal broadening of spectral line profiles [Hassler et al., 1990; Banerjee et al., 2009; Bemporad, Abbo, 2012; Chelpanov et al., 2016a]. Nonetheless, when analyzing real observational data, difficulties arise in separating the possible contribution of Alfvén waves to such a signal from the contribution of other physical mechanisms that can affect the change in the spectral line width [De Pontieu et al., 2015; Chelpanov, Kobanov, 2022]. Srivastava et al. [2017] have proposed a method for directly observing propagation of torsional Alfvén waves along the plane of the sky. They observed spatially resolved halves of a magnetic flux tube, in which oppositely directed and alternating Doppler velocities were recorded. Morton et al. [2015], when observing the lower corona in the regions of open field lines, using Coronal Multi-Channel Polarimeter (CoMP) data, noted an increased oscillation power in the 3–5 mHz range. They also observed propagation of line-of-sight velocity fluctuations along coronal structures. The same waves were observed in EUV lines as a direct displacement of the structures visible in the

images. The authors called these oscillations alfvénic waves, i.e. such waves that are similar to Alfvén waves in their properties (transverse, propagating at a near-Alfvén velocity), but are not Alfvén waves. We think that this term does not have a clearly defined physical meaning, and the waves observed by the CoMP instrument are the kink fast mode of waves in coronal structures. Note also that a shear Alfvén wave cannot exist in highly structured plasma of the solar corona since even in the case of straight field lines the shear plasma motions across the field will lead to a change in its density already in the linear approximation.

In the magnetosphere, as mentioned above, the definition of Alfvén wave is not as rigorous as in solar physics. A wave observed in the magnetosphere is classified as Alfvén if it is monochromatic and has a near-Alfvén frequency and a small longitudinal magnetic field component. Most ULF waves in Earth’s magnetosphere are interpreted as Alfvén waves [Anderson et al., 1990, 1992]. In geophysics, it is customary to divide observed Alfvén waves into two main types of field line oscillations: toroidal and poloidal (Figure 6). If the magnetic field oscillations occur in the radial direction and the radial component of the wave magnetic field exceeds the azimuthal one, such oscillations are called poloidal or poloidally polarized. Otherwise, when the azimuthal magnetic field component significantly exceeds the radial one, the oscillations are called toroidal or toroidally polarized [McPherron, 2005].

Toroidal waves result from the Alfvén resonance with fast mode or from wave transformation from poloidal to toroidal due to magnetic field curvature and inhomogeneity [Leonovich, Mazur, 1993; Leonovich et al., 2015]. Poloidal waves arise from resonant interactions with high-energy charged particles due to the development of plasma instabilities [Glassmeier et al., 1999; Kostarev, Mager, 2017], from the occurrence of alternating currents during substorm injection of particles into the magnetosphere [Guglielmi, Zolotukhina, 1980; Mager, Klimushkin, 2008], from amplifications of field-aligned currents and ionospheric electrojets [Kleimenova et al., 1995], as well as from the interaction of various ULF modes in a curved magnetic field in an inhomogeneous plasma [Pokhotelov et al., 1985], for example, from coupling of Alfvén and drift-compressional modes [Rubtsov et al., 2018b, 2020]. Satellite and ground-based observations are used to determine the generation mechanism in each particular case.

Oscillations with small azimuthal wave numbers m are usually toroidally polarized and propagate to the pole [Yeoman et al., 2012]. On the other hand, waves with large m are more likely to have poloidal polarization

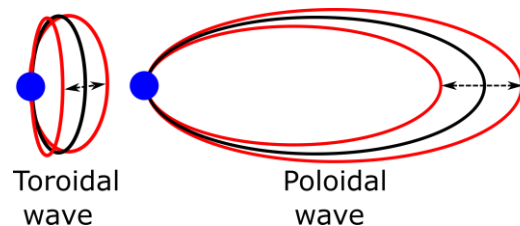


Figure 6. Toroidal and poloidal modes of Alfvén waves in the magnetosphere [Mikhailova et al., 2020a]

[James et al., 2016]. For the waves with $m \sim 10 \div 20$, the oscillations can be both poloidal and toroidal in each individual case [Hao et al., 2014]. The toroidal and poloidal oscillations can be both long-period (10–600 s) and short-period (0.2–10 s) [Mikhailova et al., 2020a, b].

Not all ULF oscillations occur on the Earth surface. Waves with $m > 10$ experience strong damping due to the screening properties of the ionosphere and are not observed on Earth. A number of studies have shown that, in comparison with ground-based observations, such oscillations are more often observed in space and in the ionosphere [Ponomarenko et al., 2003; Yagova et al., 2015]. Due to the appearance of currents in the ionosphere and the finite conductivity of the atmosphere, the wave magnetic field exponentially attenuates on a scale of $1/k$ when passing through the ionosphere, where k is the wave vector component across field lines [Hughes, Southwood, 1976a, b]. Thus, the parallel wave vector component turns out to be purely imaginary and almost equal in absolute value to the transverse wave number.

Alfvén waves can accelerate or decelerate magnetospheric charged particles by interacting with them through ion-cyclotron, drift, bounce-drift resonances, as well as resonances of other types [Cornwall et al., 1965; Borovsky, 1993; Ren et al., 2018, 2019]. The field-aligned electric field of Alfvén waves, which can be taken into account in the kinetic approach, can accelerate cold electrons, contributing to their precipitation into the atmosphere [Kostarev et al., 2021], which leads to variations in the intensity of auroras [Keiling et al., 2002; Yamamoto et al., 1988].

Thus, in both media, it is the Alfvén waves that are an essential link for many processes. As in the case of the fast mode, there is an obvious significant difference in the possibility of observing Alfvén oscillations in different media.

3.4. Wave resonators

Another similarity between the magnetosphere and a solar active region is the presence of resonators for MHD waves. However, if in the case of the magnetosphere such a resonator is the entire magnetosphere as a whole or its magnetic shells, in the solar corona resonators of MHD waves are coronal loops — thin and long magnetic flux tubes, the density and temperature inside of which differ significantly from the surrounding plasma. Due to the difference between the sound and Alfvén velocities inside the loop and in the background plasma, the coronal loop acts as a waveguide for MHD waves.

The main structural elements of the solar corona are coronal loops, which are long, loop-like structures elongated along the magnetic field and filled with plasma that glows brightly in EUV lines (Figure 7). The increased intensity of EUV radiation of coronal loops is usually observed in several lines at once and indicates an increased plasma density inside the loops since the EUV radiation of the solar corona is optically thin and its intensity is proportional to the square of the plasma density. Due to the increased density, the Alfvén velocity inside the coronal loop turns out to be lower than that in the background plasma, which makes the coronal loop a resonator for MHD waves.



Figure 7. Solar corona image in the 171 Å line, taken by SDO/AIA on November 18, 2014

The theory of waves in such a resonator was independently developed by Zaitsev and Stepanov [1975] and Edwin and Roberts [1983], who considered MHD waves in a coronal loop, using its simplified model — the magnetic cylinder as an example. In this model, plasma inside and outside the cylinder is assumed to be homogeneous, whereas on the surface of the cylinder there is a sharp jump in plasma parameters: pressure, temperature, density, and absolute value of the magnetic field. In such a magnetic cylinder, there may be a number of modes that can be divided into surface and body waves according to their localization. In the former, the disturbance is concentrated at the boundary of the cylinder; in the latter, it is distributed in its volume. In addition, the modes are grouped into trapped and leaky waves. In trapped modes, the amplitude of disturbances in the external environment decreases exponentially, and the wave is trapped inside the resonator. In the case of leaky modes, this does not happen, and the waves flow out into the external environment, and the resonator itself plays the role of an antenna for MHD waves. In what follows, we will restrict our consideration to trapped body modes.

Linearization of MHD equations and imposition of boundary conditions for the case of trapped waves in a magnetic flux tube [Edwin, Roberts, 1983] lead to the following dispersion equation for magnetosonic waves:

$$\begin{aligned} \rho_0 (k_z^2 v_{A0}^2 - \omega^2) \kappa_e \frac{K'_m(\kappa_e a)}{K_m(\kappa_e a)} &= \\ = \rho_e (k^2 v_{Ae}^2) \kappa_0 \frac{I'_m(\kappa_0 a)}{I_m(\kappa_0 a)}, \end{aligned} \quad (7)$$

where

$$\kappa_e^2 = \frac{(k_z^2 c_e^2 - \omega^2)(k_z^2 v_{Ae}^2 - \omega^2)}{(c_e^2 + v_{Ae}^2)(k_z^2 c_{Te}^2 - \omega^2)}, \quad c_{Te}^2 = \frac{c_e^2 v_{Ae}^2}{c_e^2 + v_{Ae}^2}, \quad (8)$$

$$\kappa_0^2 = \frac{(k_z^2 c_0^2 - \omega^2)(k_z^2 v_{A0}^2 - \omega^2)}{(c_e^2 + v_{A0}^2)(k_z^2 c_{T0}^2 - \omega^2)}, \quad c_{T0}^2 = \frac{c_0^2 v_{A0}^2}{c_0^2 + v_{A0}^2}. \quad (9)$$

Here $I_m(x)$, $K_m(x)$, $I'_m(x)$, $K'_m(x)$ are modified Bessel

functions of order of m and their derivatives with respect to the argument; v_A , c are Alfvén and sound velocities; c_T is the tube velocity (the group velocity of a slow magnetosonic wave in a homogeneous plasma at a small angle to the field); ρ is the plasma density; a is the transverse radius of magnetic flux tube; k_z , k , m are longitudinal, radial, and azimuthal wave numbers respectively. The indices e , 0 denote parameters in the external and internal environments.

When the conditions $\kappa_e^2 > 0$, $\kappa_0^2 = -k_r^2 < 0$ hold, volume modes trapped inside the magnetic flux tube are obtained. In this case, perturbation of the plasma parameters is as follows:

$$\xi(r, \theta, \varphi) = \begin{cases} A_0 J_m(k_r r) e^{i(m\varphi + k_z - \omega t)}, & r \leq a \\ A_e K_m(\kappa_e r) e^{i(m\varphi + k_z - \omega t)}, & r > a \end{cases}, \quad (10)$$

where $J_n(x)$ is the Bessel function of the first kind; A_0 , A_e are the constants such that the continuity of perturbation ξ at the tube boundary is not violated ($r=a$). Further, we restrict ourselves to considering these modes.

Dispersion relation (7) defines two groups of modes: fast and slow. For coronal plasma conditions with small β , the phase velocity of slow modes is between the tube and sound speed inside the tube $c_{T0} > \omega/k > c_0$. Fast modes, in turn, have a phase speed in the interval between the internal and external Alfvén speeds $v_{A0} > \omega/k > v_{Ae}$. Also noteworthy is that a magnetic flux tube with a reduced density $v_{Ae} < v_{A0}$ ceases to be a waveguide for fast magnetosonic waves and there are no trapped fast body modes in it.

The spatial structure of a particular magnetic flux tube is determined by three wave numbers: k_z , k_r , m . The character of the wave modes depends especially strongly on the azimuthal wave number m . At $m=0$, the disturbances are transverse contractions and expansions of the coronal loop, with the area of its cross-section changing, and the position of the axis remaining constant. Such modes are commonly referred to as radial or sausage modes [Nakariakov et al., 2003; Aschwanden et al., 2004]. At $m=1$, a kink mode is formed in which the longitudinal axis of the structure shifts, and its cross-section changes slightly [Nakariakov et al., 2021]. The modes with $m > 1$ are called fluting modes [Soler, 2017; Shukhobodskaya et al., 2021]. In addition, the wave modes of magnetic cylinder are divided according to the nature of disturbance into Alfvén, fast, and slow magnetoacoustic modes. In coronal structures, the sausage and kink (fast) modes, as well as the sausage slow mode, have received the most study. The last one is more often referred to in the literature as a longitudinal slow MHD wave. Dispersion properties of MHD waves in coronal structures depend very much on wave numbers, and their oscillation periods are sensitive to the geometric dimensions of the resonator structure. For instance, the period of longitudinal slow mode oscillations and kink fast mode waves is determined by the length of the structure, whereas the period of sausage fast mode oscillations of coronal loop depends mainly on its transverse dimensions. The latter is explained by a very strong dispersion of the sausage fast mode and by the presence

of a cutoff in the longitudinal wave number, due to which global sausage oscillations can exist in the coronal loop only with a wavelength of the order of the transverse size of the structure or shorter.

Unlike the ideal magnetic cylinder, real coronal loops have curvature, and plasma parameters inside the loop, such as magnetic field strength and density, depend on the distance along the axis of the structure. Yet, considering this fact does not qualitatively change the composition of the wave modes, although it causes some changes in the natural frequency spectrum. For example, the influence of the magnetic field curvature on kink oscillations in coronal loops was discussed in the review [van Doorselaere et al., 2009]. Numerical simulation the authors carried out has demonstrated that the coronal loop curvature leads to coupling of azimuthal modes (radial, kink, and fluting) due to axial symmetry breaking. The oscillation frequency in the first order of precision does not depend on the radius of curvature, and relative variations in oscillation frequencies are of the order $\sim \varepsilon^2$, where ε is the ratio of the transverse radius of loop to its radius of curvature. Thus, for typical coronal loops, this correction does not exceed 6%. Moreover, in a coronal loop curved in the form of a semicircle there are two preferred directions of polarization of kink oscillations, which result in the formation of two eigenmodes with horizontal and vertical polarizations (similar to toroidal and poloidal modes of magnetospheric oscillations).

The magnetosphere is a cavity in the solar wind and is separated from the solar wind by a rather sharp boundary — the magnetopause. Such a structure of the magnetosphere allows us to consider it as a huge resonator, and the resonator's eigenmodes are interpreted as MHD oscillations. On the one hand, wave propagation along field lines has two sharp boundaries — the ionosphere of the Northern and Southern hemispheres. Standing waves are formed on closed field lines [Leonovich, Mazur, 2016]. There may be local resonators along field lines. For instance, due to the magnetic field inhomogeneity along field lines and the presence of heavy ion admixture, an equatorial resonator may be developed. Waves standing along field lines are formed in the resonator; the size of such a resonator is determined by the heavy ion number density [Guglielmi et al., 2000, 2001; Klimushkin et al., 2010; Mikhailova et al., 2020a; Mikhailova et al., 2022a].

On the other hand, due to the plasma inhomogeneity inside the magnetosphere, volume resonators for ULF waves can evolve. Such waveguides appear in regions where the plasma parameters change abruptly, for example, at the plasmopause [Dmitrienko, Mazur, 1992] and in the partial ring current region [Denton, Vetoulis, 1998; Klimushkin, 1998; Vetoulis, Chen, 1994]. In this region, the Alfvén velocity has a minimum and a waveguide is formed in which a wave trapped in the radial direction propagates azimuthally. In such a waveguide, both Alfvén waves and fast magnetoacoustic mode can propagate. In the case of heavy ion admixture, the resonator can be bounded both in the radial direction and in the direction along the magnetic field. It is a torus encircling Earth along

the geomagnetic equator (Figure 8) [Mikhailova et al., 2020b]. The existence of transverse Alfvén resonators has been confirmed by satellite observations [Mager et al., 2018].

4. CLASSIFICATION OF WAVES IN THE MAGNETOSPHERE

Unlike the variety of wave phenomena on the Sun that do not have a single morphological classification, magnetospheric waves, which were originally observed by ground-based magnetometers and were termed geomagnetic pulsations, have a generally accepted classification. Sources of the waves can be external processes such as magnetic storms or interplanetary shock waves, as well as various internal magnetospheric instabilities [Menk, 2011].

All geomagnetic pulsations are divided into two classes: Pc pulsations continuous, characterized by a quasi-sinusoidal structure and a stable spectrum, and irregular or pulsed pulsations Pi having the form of separate bursts. In turn, each of these classes is subdivided into several subclasses depending on frequency (see Table) [Jacobs et al., 1964; Troitskaya, Guglielmi, 1969]. New experimental data often pushes for a revision of this classification, which is only partially based on physical differences, yet it remains widely accepted.

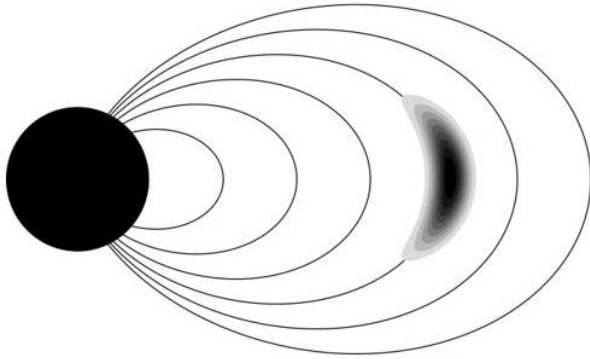


Figure 8. Amplitude distribution of a short-period wave. The wave is bounded in the radial direction and along the magnetic field and is traveling in the azimuthal direction [Mikhailova et al., 2020b]

Classification of geomagnetic pulsations

	Periods, s	Frequencies, mHz
Pulsations continuous, Pc		
Pc1	0.2–5	200–5000
Pc2	5–10	100–200
Pc3	10–45	22–100
Pc4	45–150	6.7–22
Pc5	150–600	1.7–6.7
Pulsations irregular, Pi		
Pi1	1–45	22–1000
Pi2	45–150	6.7–22

Detailed information on pulsations of different types can be found in [Mikhailova et al., 2022a] (Pc1), [Yagova et al., 2015] (Pc2–3), [Zong et al., 2017] (Pc3–5). The oscillations of the lowest frequency part have a wavelength of about thousands of kilometers, and their characteristic scale is comparable to the size of the magnetosphere itself. Further, we will focus on Pc4 and Pc5 pulsations since MHD waves in the outer magnetosphere and in the solar atmosphere fall into this frequency range.

5. WAVE OBSERVATION FACILITIES

Since information about the processes occurring in the solar atmosphere is currently available only from observations of electromagnetic radiation reaching Earth, the main methods of radiation research consist in analyzing images taken with the aid of narrowband filters, studying spectral characteristics of radiation, and analyzing brightness curves of the total flux in various ranges of the electromagnetic spectrum.

Optical, ultraviolet, X-ray, and radio telescopes are employed to study wave phenomena on the Sun, which capture images of the full solar disk, individual active regions and structures. The instruments currently in operation can observe both the total radiation (brightness curves and spectra) from the entire Sun and spatially resolved images of individual layers of the solar atmosphere. The latter are very important for studying MHD waves since they can observe wavefronts, record their velocity and direction of propagation.

In Earth’s magnetosphere, *in situ* measurements are mainly carried out by satellites equipped with magnetic and electric field sensors, as well as instruments for detecting charged particle fluxes and plasma parameters. Remote sensing of the state of the magnetosphere can partially be implemented using a wide network of ground-based magnetometers [Pilipenko, 1990; Kleimenova, 2007; Guglielmi, Potapov, 2021; Gjerloev, 2012]. Yet, some wave phenomena remain inaccessible to detection on the Earth surface due to the ionosphere screening effect [Hughes, Southwood, 1976a]. Individual wave processes occurring in the magnetosphere reflect in auroral pulsations [Motoba et al., 2021], as well as in plasma variations in the upper ionosphere observed by coherent decameter radars [James et al., 2016], and in total electron content oscillations measured by global navigation satellite systems [Pilipenko et al., 2014]. Remote sensing of near-Earth space is possible in UV, X-ray, and radio bands from satellites in polar orbits. An example of such spacecraft is the Imager for Magnetopause-to-Aurora Global Exploration (IMAGE) [Burch, 2000], as well as the future Solar wind-Magnetosphere-Ionosphere Link Explorer (SMILE) mission [Branduardi-Raymont et al., 2021].

5.1. Observing the Sun in the optical range

Optical astronomical observations are usually divided into spectral observations and imaging observations. In some cases, these two types of observations can be combined, for example, by scanning an image by the spectrograph slit in the direction perpendicular to the slit. How-

ever, for such combined observations we have to sacrifice the temporal and spatial resolution of resulting data.

Two-dimensional images provide information about morphological properties of objects. Using such data, we can identify waves propagating in the image plane, say, in coronal structures [Nakariakov et al., 2005]. Fluctuations in brightness in a separate point in such data may indicate a wave propagating along a line of sight perpendicular to the plane of the sky [Kobanov, Chelpanov, 2019].

Spectral observations usually impose limitations on observation of two-dimensional structures; however, analyzing the behavior of spectral lines provides information on line-of-sight plasma motion, as well as on magnetic field characteristics. Simultaneous observation in two or more spectral lines of the optical range makes it possible to study the plasma parameters in different layers of the solar atmosphere and thus to observe manifestations of vertically propagating wave.

Optical observations with ground-based telescopes are limited to the visible range, near ultraviolet, and parts of the infrared spectrum. Nevertheless, due to the fact that ground-based instruments are cheaper to design, build, and maintain as compared to space telescopes, they are widely used in solar physics, in particular in Russia. For example, there are solar observatories in Primorsky Krai (Ussuriysk Astrophysical Observatory of the Far Eastern Branch of the Russian Academy of Sciences [Baranov et al., 2008]), in Crimea (Crimean Astrophysical Observatory of the Russian Academy of Sciences [Gopasyuk, 2016]), in the Irkutsk Region and the Republic of Buryatia (Baikal Astrophysical Observatory, Sayan Solar Observatory [Kovadlo et al., 2016; Kobanov, Makarchik, 2002]). A large solar telescope with a mirror 3 m in diameter is planned to be built in Sayan Solar Observatory [Grigoriev et al., 2020].

Spatial resolution of instruments plays an important role in solar observations. In ground-based observations, it is limited, first of all, not by the diffraction limit of the optical scheme but by Earth's atmosphere, which distorts and blurs images. Thus, ground-based telescopes can be used to calculate the resolution of a detail with an angular size slightly smaller than 1 arcsec, which corresponds to a distance of ~ 770 km on the Sun's surface. The typical resolution of a space telescope can provide a twofold improvement in this result. However, it is possible to circumvent the limitations imposed by Earth's atmosphere by using adaptive optics, which compensates for the wavefront distortions. The highest resolution thus obtained was ~ 30 km [Rimmele et al., 2020].

5.2. Observing the solar corona in the EUV range

Observations from balloons and spacecraft (e.g., Solar and Heliospheric Observatory SOHO or Solar Dynamics Observatory SDO) expand the observable spectral range to extreme ultraviolet and X-rays, which is important when exploring the solar corona that emits in these ranges, being heated to millions of kelvins. The lines associated with atomic transitions of multiply ionized iron are most often used to observe the solar corona

in EUV. For instance, the Atmospheric Imaging Assembly onboard SDO (SDO/AIA) observes the solar corona in six EUV lines corresponding to coronal plasma with temperatures from $0.7 \cdot 10^6$ K (171 Å) to $\sim 10^7$ K (131 and 94 Å) [Lemen et al., 2012]. At each wavelength, SDO/AIA takes a full-solar disk image with a time resolution of 12 s and a spatial resolution of ~ 0.6 arcsec/pixel. The optical resolution in this case is ~ 1 arcsec. The high spatial resolution combined with the high sensitivity allows us to confidently detect MHD waves by brightness variations and displacements of individual coronal structures, and simultaneous observations in several temperature channels make it possible to estimate the temperature and density of coronal loops, for example, by calculating the differential emission measure (see, e.g., [Aschwanden, 2002; Plowman et al., 2013; Hannah, Kontar, 2012]).

In addition to the imaging instruments, EUV spectral observations are made using such instruments as SOHO/SUMER, Hinode/EIS, and IRIS. Spectral line shifts make it possible to directly measure plasma flow velocities along the line of sight; and their non-thermal broadening give an insight into the energy of small-scale, spatially unresolved motions, including those associated with Alfvén waves.

5.3. Observing the Sun in the radio range

Another important source of information about coronal plasma is microwave observations. Unlike EUV lines, microwave radiation is formed not by atomic transitions of individual elements but by free electrons. Properties of this radio emission depend not only on plasma temperature and density but also on coronal magnetic field strength and direction, which makes multiwave observations a unique tool for diagnosing coronal plasma. Thus the polarization of thermal free-free radiation makes it possible to estimate the line-of-sight coronal magnetic field component [Gelfreikh, Shibasaki, 1999], and the gyroresonance emission of active regions permits measuring the magnetic field modulus at the base of the solar corona [Zheleznyakov, Zlotnik, 1980]. The gyrosynchrotron emission that occurs in solar flares also makes it possible to monitor the dynamics of the magnetic field and some other plasma parameters directly at the flare site, and, in the case of spatially resolved observations, to map the distribution of plasma parameters in a flaring active region.

A feature of observations in the radio range is a high (compared to the available EUV data) time resolution of observations, but relatively modest spatial resolution. The latter imposes serious limitations on the use of the data for diagnosing the spatial configuration of wave disturbances. At the same time, the highest time resolution facilitates studying the oscillations with periods of several seconds, which is especially important when examining sausage oscillations whose characteristic periods range from a few seconds to several tens of seconds. The point is that the highest resolution of existing regular EUV observations is 12 s (for SDO/AIA), which is insufficient to detect oscillations with periods of the order of 10 s or shorter.

The height of formation of microwave emission strongly depends on frequency and that is why new generation radioheliographs, such as Siberian Radioheliograph (SRH) [Altyntsev et al., 2020], Mingantu Spectral Radioheliograph (MUSER) [Yan et al., 2021], and Expanded Owens Valley Solar Array (EOVSA), can observe the solar atmosphere simultaneously at different heights, thereby recording vertical wave propagation between different chromospheric and solar corona layers. Such a solar image in the microwave range is shown in Figure 9.

Another instrument that makes regular observations of the Sun with spatial resolution in the microwave range is the Academy of Sciences Radio Telescope – 600 (RATAN-600). It takes one-dimensional scans of the solar disk when the Sun due to Earth rotation passes through the instrument’s directional pattern.

5.4. *In situ* observations of the Sun

Direct *in situ* observations of coronal plasma are fraught with formidable technical difficulties due to the high temperature of the solar atmosphere and the extremely powerful solar flux near the Sun. Only in recent years has an attempt been made to perform *in situ* measurements in the solar corona with NASA’s Parker Solar Probe [Fox et al., 2016], which has already carried out measurements inside the corona [<https://www.nasa.gov/feature/goddard/2021/nasa-enters-the-solar-atmosphere-for-the-first-time-bringing-new-discoveries>] and will eventually approach the Sun at a distance of less than ten solar radii, whereas ground-based and orbital observatories observe the Sun from a distance twenty times longer.

5.5. Satellite observations in Earth’s magnetosphere

Satellite observations make it possible to measure magnetic field vector oscillations at the location of the

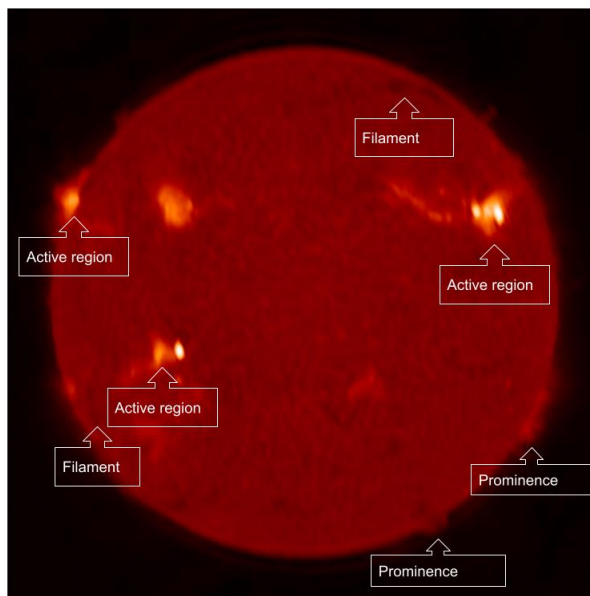


Figure 9. Radio image of the Sun taken by SRH at a frequency of 9.8 GHz on February 3, 2022. Active regions, filaments, and prominences are marked off

spacecraft. The standard procedure is the transition to a local orthogonal curved coordinate system in which one of the axes is directed along the magnetic field line. The remaining coordinate axes are the radial axis, directed from Earth, and the azimuth axis, completing the orthogonal system. Such a coordinate system is convenient for studying ULF waves as it can separate transverse and longitudinal waves. Oscillations of the radial magnetic field component are attributed to poloidal Alfvén waves; and the azimuthal one, to toroidal waves [Klimushkin et al., 2004]. Oscillations of the longitudinal component (compressional waves) are treated as drift compressional modes [Chelpanov et al., 2016b; Rubtsov et al., 2018a] and drift mirror modes [Soto-Chavez et al., 2019] considered in the kinetic theory. The best theoretical description of compressional waves is still under discussion [Takahashi et al., 2022]. Besides, observations show that oscillations generally occur in all magnetic field components at a time. The frequently detected transverse waves have therefore a mixed poloidal/toroidal polarization [Oimatsu et al., 2018a; Rubtsov et al., 2021]. The transverse waves well described in the framework of MHD were observed to have a compressional component, albeit weak. If a satellite stays near a node along a field line, the compressional component may even be dominant.

Determining the longitudinal wave structure involves finding out to which harmonic it corresponds. For odd harmonics, the node of magnetic field oscillations is located on the magnetic equator, and for even harmonics the nodes are shifted symmetrically from it to the Northern and Southern hemispheres. To determine the parity of the harmonic observed, the phase delay is studied between oscillations of the dominant magnetic field component and the electric field component orthogonal to it. Depending on whether a wave is observed to the north or south of the magnetic equator, fluctuations in the electric field will be ahead or behind the fluctuations in the magnetic field by 90° [Korotova et al., 2016].

Simultaneous measurement of particle fluxes at the same space point, where magnetic field oscillations occur, allows us to conclude that the waves interact with particles: to determine the resonant particle population and to assume a source of energy for generation. Protons used to be generally considered as resonant particles [Shi et al., 2018], but now cases of resonant interactions with electrons [Chelpanov et al., 2019; Mikhailova et al., 2022b] and oxygen ions [Oimatsu et al., 2018b] have been found. The energy of resonant particles in this case usually ranges from a few to hundreds of kiloelectronvolts. There is, however, always a problem of separating spatial and temporal variations for one satellite. The resonant wave-particle interaction usually occurs during substorm injections, magnetic storms, or when an interplanetary shock wave passes through the magnetosphere [McPherron, 2005; Zong, 2022].

In recent years, ULF waves have been intensively studied due to the launch of many satellite missions, including those consisting of several closely spaced spacecraft. Among such successful magnetospheric

missions are Time History of Events and Macroscale Interactions during Substorms (THEMIS) [Angelopoulos, 2008], Van Allen Probes [Mauk et al., 2013], Magnetospheric MultiScale (MMS) [Burch et al., 2016], and Arase [Miyoshi et al., 2018]. The presence of a large number of spacecraft at a time has opened up opportunities for long-term continuous monitoring of the magnetosphere simultaneously in different sectors. Figure 10 exemplifies the observation of a poloidal Alfvén wave for 15 hrs in the dayside magnetosphere by Van Allen Probes, THEMIS, and GOES satellites. In this case, it was possible to trace the dynamics of the wave-particle interaction during a series of substorm injections and to identify the complete spatial structure of the wave. It was shown that the ULF wave was generated by the gradient instability formed during the magnetic storm recovery phase, and effects of the substorm injections were insignificant [Rubtsov et al., 2021]. In other cases, the “pearls-on-a-string” configuration of five THEMIS satellites made it possible to determine compressional-wave propagation parameters [Constantinescu et al., 2009; Rubtsov et al., 2018a]. Multipoint observations were used when analyzing the excitation of ULF waves due to the impact of interplanetary shock waves on the magnetosphere [Zong et al., 2009; Korotova et al., 2018] and during magnetic storms [Le et al., 2017].

5.6. Radar observation of magnetospheric ULF waves

Significant progress in studying magnetospheric ULF pulsations has been achieved due to radar observations [Walker, Greenwald, 1981]. Unlike satellite and ground-based magnetometers, radars detect magnetic

field oscillations indirectly by observing variations in Doppler frequency shifts in the signal scattered by plasma inhomogeneities in the ionosphere. Periodic variations in Doppler shifts occur when, under the influence of drift in crossed magnetic and electric fields, ion velocity fluctuations develop in the horizontal direction. The wave magnetic field strength being low compared to the geomagnetic field strength, the amplitude of the velocity fluctuations is directly proportional to the wave electric field. Radars can receive a scattered signal from vast regions of the ionosphere, thereby providing data with a higher spatial resolution compared to ground-based magnetometers [Nishitani et al., 2019].

The advantages of using radars are of particular importance for ULF waves with large azimuthal wave numbers ($|m| > 20$) because due to the ionosphere screening effect they are difficult to detect in the Earth surface. This leads to the fact that a significant part of the waves that can be recorded by radars in no way appears in the data from ground-based magnetometers. Ponomarenko et al. [2003], using observational data from the Tasman International Geospace Environment Radar (TIGER), have shown that the percentage of such waves run to 46 %.

Simultaneous acquisition of data from an area whose projected dimensions along field lines on the equatorial plane are as large as several Earth radii makes it possible not only to distinguish between temporal and spatial changes in parameters of ULF waves, but also to trace transformations in their properties on a number of magnetic shells. For instance, waves with a curved front have been experimentally studied [Yeoman et al., 2012]. A disadvantage of radars in terms of ULF oscillations may be detection of only one wave component —

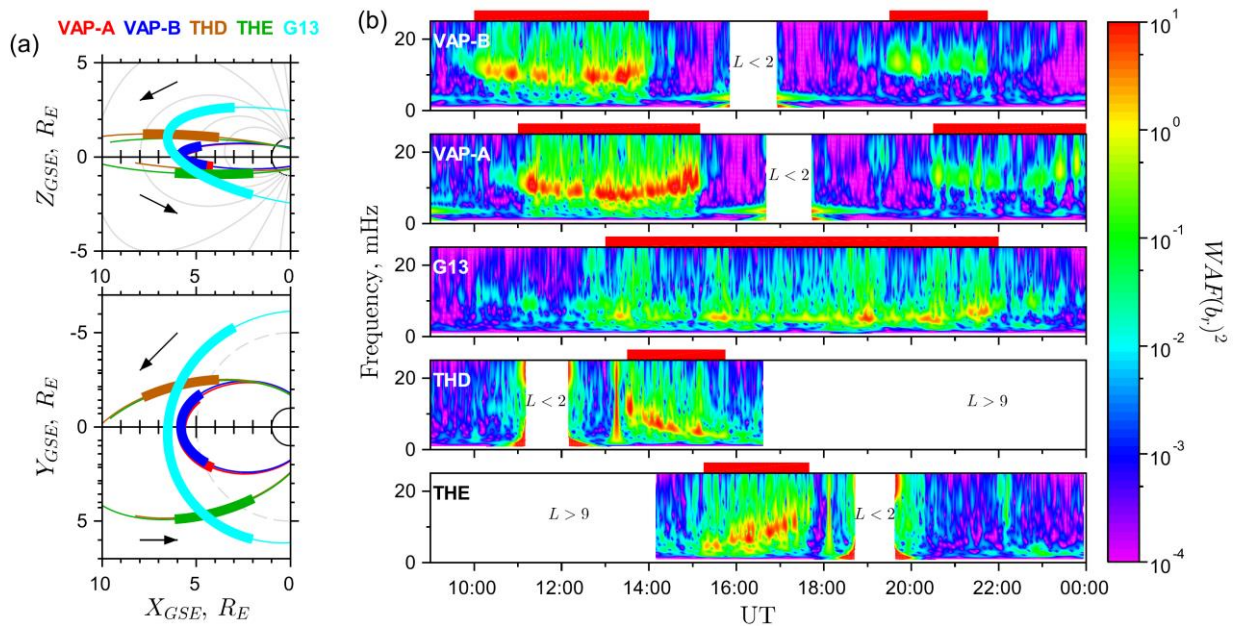


Figure 10. Pc4 and Pc5 waves in the dayside magnetosphere as observed by THEMIS (THD and THE), Van Allen Probes (VAP-A and VAP-B), and GOES (G13) satellites on February 25, 2014: (a) – satellite orbits in the meridional (top) and equatorial (bottom) planes with portions of the orbits, where the waves were observed, indicated by a thick line; (b) – wavelet spectra of the radial magnetic field component of the satellites, from top to bottom: VAP-B, VAP-A, G13, THD, THE. Red strips above each panel are the time intervals when the waves were observed

one radar can obtain data on the velocity of ionospheric plasma at a given point only in the direction of signal propagation, i.e. along the line connecting the radar and this point. This problem is solved by using pairs (or networks) of radars with overlapping fields of view. Another limitation is the time of one scan of the radar field of view. The scanning rate determines the maximum rate of the oscillations under study: the minimum wave period should be two times higher than the time resolution of the radar.

The Scandinavian Twin Auroral Radar Experiment (STARE) was among the first to be used for regular observations of ULF oscillations [Nielsen, 1982]. They receive a signal scattered by irregularities of the ionospheric E layer (90–120 km) from an area of ~ 160000 km², providing a spatial resolution of ~ 20 km. Overlapped fields of view of the two radars with different scanning directions yield the full vector of the horizontal velocity of ionospheric plasma. The data obtained by this radar system was used to examine the structure of standing Alfvén waves and to support theoretical concepts [Walker et al., 1979].

The next stage of examining ionospheric convection with radars was the use of the Super Dual Auroral Radar Network (SuperDARN) [Greenwald et al., 1995]. Unlike the STARE signal, the high-frequency SuperDARN signal is scattered by ionospheric F-layer irregularities (over 130 km above the Earth surface). In this case, there is no need to take into account such phenomena as the 90° wave polarization rotation in passing through the E layer. Electrons and ions at the F-layer heights drift at roughly the same velocity, which somewhat simplifies the interpretation of the data [Chisham et al., 2007]. Refraction typical of high frequencies in the ionosphere allows multihop paths to be employed, which enables reception of a scattered signal from long distances up to several thousand kilometers from a radar. Since the standard scanning time of the field of view, which is 1–2 min, is too long to detect short-period variations in the Doppler plasma velocity, special scanning modes are used which ensure signal reception only from a narrow field-of-view sector. This allows us to decrease the total time of one scan and increase the time resolution of data.

One of the advantages in SuperDARN is its extension to middle latitudes [Nishitani et al., 2019]. Closer to the equator during substorms, radar data is less susceptible to degradation caused by signal absorption and changes in propagation condition, associated with precipitation in the D and E layers of the ionosphere during substorms [Gauld et al., 2002].

There are no SuperDARN radars in Russia, but there is a coherent scatter radar identical to the network's radars in middle latitudes near Ekaterinburg [Berngardt et al., 2015]. The radar detects backscattered signals from distances up to 3500 km, which corresponds to 54°–78° geomagnetic latitude. Part of the time is applied to additional scanning sequence to obtain data with a higher time resolution in two or three scanning directions with a time resolution of 12 and 18 s respec-

tively. One of the versions of the additional mode is scanning in directions close to the magnetic meridian (deviation to 7°). In this mode, the radar registers fluctuations in the plasma velocity component approximately aligned with the magnetic meridian (Figure 11). The fluctuations in this direction being caused by the drift in the radial magnetic field (the direction to and from Earth), this scan mode provides information on poloidal oscillations of the magnetic field without having to separate them from toroidal ones.

6. DISCUSSION AND CONCLUSION

Plasma of Earth's magnetosphere and solar active regions have both significant differences and common features. Earth's magnetosphere and the Sun's atmosphere are a space filled with cold plasma and bounded from above and below by special surfaces, where the plasma parameter $\beta \sim 1$. In the Sun's atmosphere, this is the photosphere and chromosphere from below and the source surface, which separates the solar corona from the freely moving wind, from above; whereas in the magnetosphere, the boundary with the ionosphere from below and the magnetopause from above. In these regions, abrupt changes in plasma parameters create conditions for wave reflection and formation of resonators, and conversion of various MHD modes into each other becomes effective on these surfaces.

Similar observational manifestations of ULF waves in both media include the following.

1. Similar frequency ranges of observed oscillations (a few to thousands of mHz). In the Sun's atmosphere, most of the oscillations have periods from 10 to 600 s with some characteristic peaks in the distribution, such as three- and five-minute oscillations in the chromosphere. In Earth's magnetosphere, a similar range of periods includes standing oscillations of field lines. Their values are determined by the characteristic dimensions of the magnetosphere, as well as by plasma parameters and magnetic field strength. The periods of the oscillation modes described in the kinetic approach also fall into this range.

2. Despite the differences in the characteristic magnitudes of the magnetic field, particle density and temperature both in the solar corona and in Earth's magnetosphere, the condition $\beta \ll 1$ is met.

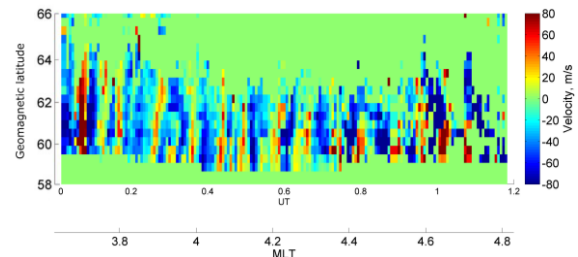


Figure 11. Plasma velocity along one of the scanning directions on December 25, 2014. Positive values correspond to the movement toward the radar (to the south). Vertical strips correspond to poloidal oscillations with a frequency of ~ 4 mHz

3. In Earth's magnetosphere, the Alfvén velocity is by about an order of magnitude higher than in the chromosphere, but is close to its value in the solar corona (~ 1000 km/s).

4. Characteristic scales of active regions in the Sun's atmosphere are close to the size of Earth's magnetosphere (~ 100000 km). As mentioned above, this is, among other things, a factor in the similarity between the ranges of periods of the observed oscillations. Transverse dimensions of inhomogeneities in both media are also similar (about 1–10 thousand km).

Among the differences between parameters of plasma of the Sun's atmosphere and the magnetosphere, the most significant is the particle density that differs by several orders of magnitude, and hence the difference in the mean free path. Due to this, plasma in the Sun's atmosphere is collisional; in the magnetosphere, collisionless. The magnetic pressure in almost all magnetospheric regions significantly exceeds the gas pressure ($\beta < 1$), whereas in the Sun's atmosphere there are regions in which the gas pressure is equal to or exceeds the magnetic pressure ($\beta \geq 1$). In the chromosphere and corona, plasma is strongly structured across the magnetic field, whereas the magnetosphere is much more homogeneous.

In studies based on both solar and magnetospheric physics, it should be borne in mind that in these regions there are differences in the terminology describing wave processes. The most significant difference is in the use of the term "Alfvén waves". Alfvén waves on the Sun are transverse oscillations of magnetic field lines and plasma frozen in them. At the same time, the compulsory condition is the absence of attendant density perturbations and hence emission intensity. This represents an obstacle to their direct observations.

In the magnetosphere, by Alfvén waves are also meant displacements of field lines and their associated plasma, yet their attendant pressure disturbances are usually neglected. The waves observed in the magnetosphere can hardly be described in pure MHD — this requires more complex approaches such as the kinetic theory. However, as practice shows, Alfvén MHD waves quite accurately describe most magnetospheric wave phenomena.

An example of successful application of unified approaches to solving problems of solar and magnetospheric physics is a series of papers [Klimushkin et al., 2017; Rubtsov et al., 2018b, 2020], where the conditions for respectively corrugation and ballooning instabilities are investigated. In [Klimushkin et al., 2017], the theory of MHD instabilities developed in magnetospheric physics was applied to conditions of disturbance generation with respect to the corrugation instability in the solar corona. For the cylindrical model, a system of coupled equations for Alfvén wave and slow magnetoacoustic mode was solved. The authors derived analytical expressions, determined the radial structure of disturbance and the dependence of the instability growth rate on wavelength in longitudinal and transverse directions. Rubtsov et al. [2018b] have applied a similar approach to magnetospheric conditions. They also defined insta-

bility criteria but for the geometry of dipole magnetic field. Rubtsov et al. [2020] also take into account the inhomogeneity across the magnetic field (a sharp drop in plasma pressure with distance away from Earth), whereas previous works considered only the inhomogeneity along it. It was shown that a certain minimum threshold value of the azimuthal wave number m (30–70 for medium parameters typical of the magnetosphere) is required for the instability to occur.

While the solar and magnetospheric physics have been studied extensively, there are still many unresolved problems. Such issues as heating of the solar corona, extreme changes in the geomagnetic field during geomagnetic disturbances, and the processes of triggering of substorms remain open and call for future research. Combining theory and observations of wave phenomena on the Sun and in the magnetosphere may help to solve these and other problems.

For instance, direct measurements of some parameters can be made in the magnetosphere (particle fluxes, electromagnetic fields) and are not available in the solar atmosphere, whereas others (space-time evolution of fast mode waves) observed on the Sun at various wavelengths cannot be directly measured in the magnetosphere.

The development of a general theory of oscillation processes, unified for media of the Sun—Earth system, seems to be promising but difficult to accomplish. Despite a number of limitations, combining theories and applying the methods of one discipline to the problems of another can probably open up new prospects for the study into waves both in the Sun's atmosphere and in Earth's magnetosphere.

The work was financially supported by RSF (Project No. 21-72-10139). Solar data in the H α line was obtained using the Unique Research Facility "Large Solar Vacuum Telescope". The radio image of the Sun was obtained using the equipment of Shared Equipment Center "Angara" [<http://ckp-rf.ru/ckp/3056>]. We gratefully acknowledge NASA's Van Allen Probes mission and C. Kletzing for providing EMFISIS data, NASA and V. Angelopoulos for THEMIS data, and U. Auster, K.-H. Glassmeier, and J. Mieth for FGM data. EUV full solar disk data was provided by the SDO research team. We and Editorial Board of the journal are grateful to A.G. Demekhov for valuable assistance in finalizing the paper during its review.

REFERENCES

- Akhiezer A.I., Akhiezer I.A., Polovin R.V., Sitenko A.G., Stepanov K.N. *Plasma electrodynamics*. Moscow, Nauka Publ., 1974, 720 p. (In Russian).
- Anderson B.J., Engebretson M.J., Rounds S.P., Zanetti L.J., Potemra T.A. A statistical study of Pc 3-5 pulsations observed by the AMPTE/CCE Magnetic Fields Experiment, 1. Occurrence distributions. *J. Geophys. Res.* 1990, vol. 95, no. A7, pp. 10495–10523. DOI: [10.1029/JA095iA07p10495](https://doi.org/10.1029/JA095iA07p10495).
- Anderson B.J., Erlandson R.E., Zanetti L.J. A statistical study of Pc 1–2 magnetic pulsations in the equatorial magnetosphere: 2. Wave properties. *J. Geophys. Res.* 1992, vol. 97, no. A3, pp. 3089–3101. DOI: [10.1029/91JA02697](https://doi.org/10.1029/91JA02697).

- Altschuler M.D., Trotter D.E., Orrall F.Q. Coronal holes. *Solar Phys.* 1972, vol. 26, iss 2, pp. 354–365. DOI: [10.1007/BF00165276](https://doi.org/10.1007/BF00165276).
- Altyntsev A.T., Lesovoi S.V., Globa M.V., Gubin A.V., Kochanov A.A., Grechnev V.V. Multiwave Siberian Radioheliograph. *Solar-Terr. Phys.* 2020, vol. 6, iss. 2, pp. 30–40. DOI: [10.12737/stp-62202003](https://doi.org/10.12737/stp-62202003).
- Anfinogentov S.A., Nakariakov V.M., Nisticò G. Decay-less low-amplitude kink oscillations: A common phenomenon in the solar corona? *Astron. Astrophys.* 2015, vol. 583, A136. DOI: [10.1051/0004-6361/201526195](https://doi.org/10.1051/0004-6361/201526195).
- Anfinogentov S.A., Stupishin A.G., Mysh'yaikov I.I., Fleishman G.D. Record-breaking coronal magnetic field in solar active region 12673. *Astrophys. J.* 2019, vol. 880, iss. 2, p. L29.
- Angelopoulos V. The THEMIS Mission. *Space Sci. Rev.* 2008, vol. 141, pp. 5–34. DOI: [10.1007/s11214-008-9336-1](https://doi.org/10.1007/s11214-008-9336-1).
- Antonsen Jr. T.M., Lane B. Kinetic equations for low frequency instabilities in inhomogeneous plasmas. *Physics of Fluids.* 1980, vol. 23, iss. 6, pp. 1205–1214. DOI: [10.1063/1.863121](https://doi.org/10.1063/1.863121).
- Aschwanden M.J. The differential emission measure distribution in the multiloop corona. *Astrophys. J.* 2002, vol. 580, no. 1, pp. L79–L83. DOI: [10.1086/345469](https://doi.org/10.1086/345469).
- Aschwanden M.J., Nakariakov V.M., Melnikov V.F. Magneto-hydrodynamic Sausage-Mode Oscillations in Coronal Loops. *Astrophys. J.* 2004, vol. 600, iss. 1, pp. 458–463. DOI: [10.1086/379789](https://doi.org/10.1086/379789).
- Baddeley L.J., Lorentzen D.A., Partamies N., Denig M., Pilipenko V.A., Oksavik K., et al. Equatorward propagating auroral arcs driven by ULF wave activity: Multipoint ground- and space-based observations in the dusk sector auroral oval. *J. Geophys. Res.: Space Phys.* 2017, vol. 122, pp. 5591–5605. DOI: [10.1002/2016JA023427](https://doi.org/10.1002/2016JA023427).
- Balthasar H. The oscillatory behaviour of solar faculae. *Solar Phys.* 1990, vol. 127, pp. 289–292. DOI: [10.1007/BF00152168](https://doi.org/10.1007/BF00152168).
- Banerjee D., Pérez-Suárez D., Doyle J.G. Broadening of SI VIII lines observed in the solar polar coronal holes. *Astron. Astrophys.* 1998, vol. 339, pp. 208–214.
- Banerjee D., Teriaca L., Doyle J.G., Wilhelm K. Signatures of Alfvén waves in the polar coronal holes as seen by EIS/Hinode. *Astron. Astrophys.* 2009, vol. 501, iss. 3, pp. L15–L18. DOI: [10.1051/0004-6361/200912242](https://doi.org/10.1051/0004-6361/200912242).
- Baranov A.V., Baranova A.V., Lazareva L.F. Peculiarities of the cross-over effect in sunspot penumbrae. Observation results. *Solar Activity and Its Impact on Earth.* 2008, vol. 11, pp. 13–23. (In Russian).
- Baumjohann W., Junginger H., Haerendel G., Bauer O.H. Resonant Alfvén waves excited by a sudden impulse. *J. Geophys. Res.* 1984, vol. 89, iss. A5, pp. 2765–2769. DOI: [10.1029/JA089iA05p02765](https://doi.org/10.1029/JA089iA05p02765).
- Bemporad A., Abbo L. Spectroscopic signature of Alfvén waves damping in a polar coronal hole up to 0.4 solar radii. *Astrophys. J.*, 2012, vol. 751, iss. 2, A110. DOI: [10.1088/0004-637X/751/2/110](https://doi.org/10.1088/0004-637X/751/2/110).
- Bergardt O.I., Kutelev K.A., Kurkin V.I., et al. Bistatic sounding of high-latitude ionospheric irregularities using a decameter EKB radar and an UTR-2 radio telescope: first results. *Radiophysics and Quantum Electronics.* 2015, Vol. 58, no. 6. P. 390–408. DOI: [10.1007/s11141-015-9614-1](https://doi.org/10.1007/s11141-015-9614-1).
- Bogdan T.J. Sunspot oscillations: A review. *Solar Phys.* 2000, vol. 192, pp. 373–394. DOI: [10.1023/A:1005225214520](https://doi.org/10.1023/A:1005225214520).
- Borovsky J.E. Auroral arc thicknesses as predicted by various theories. *J. Geophys. Res.* 1993, vol. 98, iss. A4, pp. 6101–6138. DOI: [10.1029/92JA02242](https://doi.org/10.1029/92JA02242).
- Braginsky S.I. Transport phenomena in plasma. *Plasma Phys.* 1963, vol. 2. Ed. Leontovich M.A. Moscow, Gosatomizdat, 1963, pp. 183–272. (In Russian).
- Branduardi-Raymont G., Wang C., Escoubet C.P., Sembay S., Donovan E., Dai L., et al. Imaging solar-terrestrial interactions on the global scale: The SMILE mission. *EGU General Assembly, 19–30 Apr. 2021.* 2021, EGU21-3230. DOI: [10.5194/egusphere-egu21-3230](https://doi.org/10.5194/egusphere-egu21-3230).
- Brueckner G.E., Bartoe J.-D.F. The fine structure of the solar atmosphere in the far ultraviolet. *Solar Phys.* 1974, vol. 38, iss. 1, pp. 133–156. DOI: [10.1007/BF00161831](https://doi.org/10.1007/BF00161831).
- Burch J.L. IMAGE mission overview. *Space Sci. Rev.* 2000, vol. 91, pp. 1–14. DOI: [10.1023/A:1005245323115](https://doi.org/10.1023/A:1005245323115).
- Burch J.L., Moore T.E., Torbert R.B., Giles B.L. Magnetospheric multiscale overview and science objectives. *Space Sci. Rev.* 2016, vol. 199, pp. 5–21. DOI: [10.1007/s11214-015-0164-9](https://doi.org/10.1007/s11214-015-0164-9).
- Burdo O.S., Cheremnykh O.K., Verkhoglyadova O.P. Study of ballooning modes in the inner magnetosphere of the Earth. *Bull. Russian Academy of Sciences: Physics.* 2000, vol. 64, iss. 9, pp. 1896–1900. (In Russian).
- Catto P.J., Tang W.M., Baldwin D.E. Generalized gyrokinetics. *Plasma Phys.* 1981, vol. 23, no. 7, pp. 639–650. DOI: [10.1088/0032-1028/23/7/005](https://doi.org/10.1088/0032-1028/23/7/005).
- Chelpanov A.A., Kobanov N.I. Methods for registering torsional waves in the lower solar atmosphere: Do observations support the theory? *44th COSPAR Scientific Assembly.* 16–24 July, 2022, vol. 44, p. 2502.
- Chelpanov A.A., Kobanov N.I., Chupin S.A. Search for the observational manifestations of torsional Alfvén waves in solar faculae. *Central European Astrophys. Bull.* 2016a, vol. 40, pp. 29–34.
- Chelpanov M.A., Mager P.N., Klimushkin D.Y., Mager O.V., Bergardt O.I. Experimental evidence of drift compressional waves in the magnetosphere: An Ekaterinburg coherent decameter radar case study. *J. Geophys. Res.: Space Phys.* 2016b, vol. 121, iss. 2, pp. 1315–1326. DOI: [10.1002/2015JA022155](https://doi.org/10.1002/2015JA022155).
- Chelpanov M.A., Mager P.N., Klimushkin D.Y., Mager O.V. Observing magnetospheric waves propagating in the direction of electron drift with Ekaterinburg decameter coherent radar. *Solar-Terr. Phys.* 2019, vol. 5, iss. 1, pp. 51–57. DOI: [10.12737/stp-51201907](https://doi.org/10.12737/stp-51201907).
- Chen L., Hasegawa A.A. theory of long-period magnetic pulsations: 1. Steady state excitation of field line resonance. *J. Geophys. Res.* 1974a, vol. 79, iss. 7, pp. 1024–1032. DOI: [10.1029/JA079i007p01024](https://doi.org/10.1029/JA079i007p01024).
- Chen L., Hasegawa A.A. Theory of long-period magnetic pulsations 2. Impulse excitation of surface eigenmode. *J. Geophys. Res.* 1974b, vol. 79, iss. 7, pp. 1033–1037. DOI: [10.1029/JA079i007p01033](https://doi.org/10.1029/JA079i007p01033).
- Chisham G., Lester M., Milan S.E., Freeman M.P., Britton W.A., Grocott A., et al. A decade of the Super Dual Auroral Radar Network (SuperDARN): Scientific achievements, new techniques and future directions. *Surveys in Geophys.* 2007, vol. 28, pp. 33–109 DOI: [10.1007/s10712-007-9017-8](https://doi.org/10.1007/s10712-007-9017-8).
- Constantinescu O.D., Glassmeier K.-H., Plaschke F., et al. THEMIS observations of duskside compressional Pc5 waves. *J. Geophys. Res.* 2009, vol. 114, A00C25. DOI: [10.1029/2008JA013519](https://doi.org/10.1029/2008JA013519).
- Cornwall J.M., Sims A.R., White R.S. Atmospheric density experienced by radiation belt protons, *J. Geophys. Res.* 1965, vol. 70, no. 13, pp. 3099–3111. DOI: [10.1029/JZ070i013p03099](https://doi.org/10.1029/JZ070i013p03099).

- Cranmer S.R., van Ballegooyen A.A., Edgar R.J. Self-consistent coronal heating and solar wind acceleration from anisotropic magnetohydrodynamic turbulence. *Astrophys. J. Suppl. Ser.* 2007, vol. 171, no. 2, pp. 520–551. DOI: [10.1086/518001](https://doi.org/10.1086/518001).
- Crooker N.U., Siscoe G.L., Geller R.B. Persistent pressure anisotropy in the subsonic magnetosheath region. *Geophys. Res. Lett.* 1976, vol. 3, pp. 65–68. DOI: [10.1029/GL003i002p00065](https://doi.org/10.1029/GL003i002p00065).
- De Moortel I. Longitudinal waves in coronal loops. *Space Sci. Rev.* 2009, vol. 149, iss. 1-4, pp. 65–81. DOI: [10.1007/s11214-009-9526-5](https://doi.org/10.1007/s11214-009-9526-5).
- De Pontieu B., Erdélyi R., De Moortel I. How to channel photospheric oscillations into the corona. *Astrophys. J.*, 2005, vol. 624, pp. L61–L64. DOI: [10.1086/430345](https://doi.org/10.1086/430345).
- De Pontieu B., McIntosh S.W., Carlsson M. Chromospheric Alfvénic waves strong enough to power the solar wind. *Science*. 2007a, vol. 318, iss. 5856, pp. 1574. DOI: [10.1126/science.1151747](https://doi.org/10.1126/science.1151747).
- De Pontieu B., McIntosh S., Hansteen V.H., Carlsson M., Schrijver Carolus J., Tarbell T.D., et al. A tale of two spicules: The impact of spicules on the magnetic chromosphere. *Publ. Astron. Soc. Japan*. 2007b, vol. 59, pp. S655–S662. DOI: [10.1093/pasj/59.sp3.S655](https://doi.org/10.1093/pasj/59.sp3.S655).
- De Pontieu B., McIntosh S., Martinez-Sykora J., Peter H., Pereira T.M.D. Why is non-thermal line broadening of spectral lines in the lower transition region of the sun independent of spatial resolution? *Astrophys. J. Lett.* 2015, vol. 799, no. 1, p. L12. DOI: [10.1088/2041-8205/799/1/L12](https://doi.org/10.1088/2041-8205/799/1/L12).
- Denton R.E., Vetoulis G. Global poloidal mode. *J. Geophys. Res.* 1998, vol. 103, iss. A4, pp. 6729–6739. DOI: [10.1029/97JA03594](https://doi.org/10.1029/97JA03594).
- Dmitrienko I.S., Mazur V.A. The spatial structure of quasicircular Alfvén modes of waveguide at the plasmopause: Interpretation of Pc1 pulsations. *Planetary and Space Sci.* 1992, vol. 40, No. 1, pp. 139–148. DOI: [10.1016/0032-0633\(92\)90156-I](https://doi.org/10.1016/0032-0633(92)90156-I).
- Dmitriev A.V., Suvorova A.V., Veselovsky I.S. Statistical Characteristics of the Heliospheric Plasma and Magnetic Field at the Earth's Orbit during Four Solar Cycles 20–23. *Handbook on Solar Wind: Effects, Dynamics and Interactions*. Ed. Hans E. Johannson. New York: NOVA Science Publishers, Inc., 2009. pp. 81–144. DOI: [10.48550/arXiv.1301.2929](https://doi.org/10.48550/arXiv.1301.2929).
- Eastmann T.E., Frank L.A. Observations of high-speed plasma flow near the Earth's magnetopause: Evidence for reconnection? *J. Geophys. Res.* 1982, vol. 87, iss. A4, pp. 2187–2201. DOI: [10.1029/JA087iA04p02187](https://doi.org/10.1029/JA087iA04p02187).
- Edwin P.M., Roberts B. Wave propagation in a magnetic cylinder. *Solar Phys.* 1983, vol. 88, iss. 1-2, pp. 179–191. DOI: [10.1007/BF00196186](https://doi.org/10.1007/BF00196186).
- Feldman U., Dammasch I.E., Wilhelm K. The morphology of the solar upper atmosphere during the sunspot minimum. *Space Sci. Rev.* 2000, vol. 93, pp. 411–472. DOI: [10.1023/A:1026518806911](https://doi.org/10.1023/A:1026518806911).
- Fox N.J., Velli M.C., Bale S.D., Decker R., Driesman A., Howard R.A., et al. The Solar Probe Plus Mission: Humanity's first visit to our star. *Space Sci. Rev.* 2016, vol. 204, pp. 7–48. DOI: [10.1007/s11214-015-0211-6](https://doi.org/10.1007/s11214-015-0211-6).
- Ganushkina N.Y., Liemohn M.W., Dubyagin S. Current systems in the Earth's magnetosphere. *Rev. Geophys.* 2018, vol. 56, pp. 309–332. DOI: [10.1002/2017RG000590](https://doi.org/10.1002/2017RG000590).
- Gauld J.K., Yeoman T.K., Davies J.A., Milan S.E., Honary F. SuperDARN radar HF propagation and absorption response to the substorm expansion phase. *Ann. Geophys.* 2002, vol. 20, pp. 1631–1645. DOI: [10.5194/angeo-20-1631-2002](https://doi.org/10.5194/angeo-20-1631-2002).
- Gelfreikh G.B., Shibasaki K. Radio Magnetography of solar active regions using radio observations. *Magnetic Fields and Solar Processes ESA Special Publication*. Ed. A. Wilson et al., 1999, p. 1339.
- Gjerloev J.W. The SuperMAG data processing technique. *J. Geophys. Res.* 2012, vol. 117, iss. A9, A09213. DOI: [10.1029/2012JA017683](https://doi.org/10.1029/2012JA017683).
- Glassmeier K.-H., Buchert S., Motschmann U., Korth A., Pedersen A. Concerning the generation of geomagnetic giant pulsations by drift-bounce resonance ring current instabilities. *Ann. Geophys.* 1999, vol. 17, iss. 3, pp. 338–350. DOI: [10.1007/s00585-999-0338-4](https://doi.org/10.1007/s00585-999-0338-4).
- Glassmeier K.-H., Mager P.N., Klimushkin D.Y. Concerning ULF pulsations in Mercury's magnetosphere. *Geophys. Res. Lett.* 2003, vol. 30, iss. 18, p. 1928. DOI: [10.1029/2003GL017175](https://doi.org/10.1029/2003GL017175).
- Gopasyuk O.S. Studies of the Sun in Crimea. *Bull. Crimean Astrophys. Observatory*. 2016, vol. 112, pp. 126–132. (In Russian).
- Greenwald R.A., Baker K.B., Dudeney J.R., Pinnock M., Jones T.B., Thomas E.C., et al. DARN/SuperDARN. *Space Sci. Rev.* 1995, vol. 71, iss. 1, pp. 761–796. DOI: [10.1007/BF00751350](https://doi.org/10.1007/BF00751350).
- Grigoryev V.M., Demidov M.L., Kolobov D.Yu., Pulyaev V.A., Skomorovsky V.I., Chuprakov S.A. Project of the large solar telescope with mirror 3 m in diameter. *Solar-Terr. Phys.* 2020, vol. 6, iss. 2, pp. 14–29. DOI: [10.12737/stp-62202002](https://doi.org/10.12737/stp-62202002).
- Guglielmi A.V. Diagnostics of the magnetosphere and interplanetary medium by means of pulsations. *Space Sci. Rev.* 1974, vol. 16, pp. 331–345. DOI: [10.1007/BF00171562](https://doi.org/10.1007/BF00171562).
- Guglielmi A.V., Dobnya B.V. Hydromagnetic emission of interplanetary plasma. *JETP Lett.* 1973, vol. 18, no. 10, pp. 353–355.
- Guglielmi A.V., Potapov A.S. Influence of the interplanetary magnetic field on ULF oscillations of the ionospheric resonator. *Cosmic Res.* 2017, vol. 55, pp. 248–252. DOI: [10.1134/S0010952517030042](https://doi.org/10.1134/S0010952517030042).
- Guglielmi A.V., Potapov A.S. Frequency-modulated ULF waves in near-Earth space. *Physics-Uspekhi*. 2021, vol. 64, no. 5, pp. 452–467. DOI: [10.3367/UFNe.2020.06.038777](https://doi.org/10.3367/UFNe.2020.06.038777).
- Guglielmi A.V., Zolotukhina N.A. Excitation of Alfvén oscillations of the magnetosphere by the asymmetric ring current. *Res. on Geomagnetism, Aeronomy, and Solar Phys.* 1980, vol. 50, pp. 129–137. (In Russian).
- Guglielmi A.V., Potapov A.S., Russell C.T. The ion cyclotron resonator in the magnetosphere. *JETP Lett.* 2000, vol. 72, iss. 6, pp. 298–300. DOI: [10.1134/1.1328441](https://doi.org/10.1134/1.1328441).
- Guglielmi A., Kangas J., Potapov A. Quasiperiodic modulation of the Pc1 geomagnetic pulsations: An unsettled problem. *J. Geophys. Res.* 2001, vol. 106, iss. A11, pp. 25847–25855. DOI: [10.1029/2001JA000136](https://doi.org/10.1029/2001JA000136).
- Guglielmi A., Potapov A., Dovbnya B. Five-minute solar oscillations and ion-cyclotron waves in the solar wind. *Solar Phys.* 2015, vol. 290, iss. 10, pp. 3023–3032. DOI: [10.1007/s11207-015-0772-2](https://doi.org/10.1007/s11207-015-0772-2).
- Hannah I.G., Kontar E.P. Differential emission measures from the regularized inversion of Hinode and SDO data. *Astron. Astrophys.* 2012, vol. 539, p. A146. DOI: [10.1051/0004-6361/201117576](https://doi.org/10.1051/0004-6361/201117576).
- Hao Y.X., Zong Q.-G., Wang Y.F., Zhou X.-Z., Zhang H., Fu S.Y., et al. Interactions of energetic electrons with ULF waves triggered by interplanetary shock: Van Allen Probes observations in the magnetotail. *J. Geophys. Res.: Space Phys.* 2014, vol. 119, iss. 10, pp. 8262–8273. DOI: [10.1002/2014JA020023](https://doi.org/10.1002/2014JA020023).

- Hasegawa A. Drift mirror instability in the magnetosphere. *Phys. of Fluids*. 1969. vol. 12, iss. 12, pp. 2642–2650. DOI: [10.1063/1.1692407](https://doi.org/10.1063/1.1692407).
- Hasegawa A., Chen L. Theory of magnetic pulsations. *Space Sci. Rev.* 1974, vol. 16, pp. 347–359. DOI: [10.1007/BF00171563](https://doi.org/10.1007/BF00171563).
- Hassler D.M., Rottman G.J., Shoub E.C., Holzer T.E. Line broadening of MG X lambda lambda 609 and 625 coronal emission lines observed above the solar limb. *Astrophys. J. Lett.* 1990, vol. 348, L77. DOI: [10.1086/185635](https://doi.org/10.1086/185635).
- Hughes W.J., Southwood D.J. An illustration of modification of geomagnetic pulsation structure by the ionosphere. *J. Geophys. Res.* 1976a, vol. 81, iss. 19, pp. 3241–3247. DOI: [10.1029/JA081i019p03241](https://doi.org/10.1029/JA081i019p03241).
- Hughes W.J., Southwood D.J. The screening of micro-pulsation signals by the atmosphere and ionosphere. *J. Geophys. Res.* 1976b, vol. 81, iss. 19, pp. 3234–3240. DOI: [10.1029/JA081i019p03234](https://doi.org/10.1029/JA081i019p03234).
- Jacobs J.A., Kato Y., Matsushita S., Troitskaya V.A. Classification of geomagnetic micropulsations. *J. Geophys. Res.* 1964, vol. 69, iss. 1, pp. 180–181. DOI: [10.1029/JZ069i001p00180](https://doi.org/10.1029/JZ069i001p00180).
- James M.K., Yeoman T.K., Mager P.N., Klimushkin D.Yu. Multiradar observations of substorm-driven ULF waves. *J. Geophys. Res.: Space Phys.* 2016, vol. 121, pp. 5213–5232. DOI: [10.1002/2015JA022102](https://doi.org/10.1002/2015JA022102).
- Keiling A., Wygant J.R., Cattell C., Peria W., Parks G., Temerin M., et al. Correlation of Alfvén wave Poynting flux in the plasma sheet at (4–7) R_E with ionospheric electron energy flux. *J. Geophys. Res.* 2002, vol. 107, iss. A7, pp. SMP24-1–SMP24-13. DOI: [10.1029/2001JA900140](https://doi.org/10.1029/2001JA900140).
- Kepko L., Spence H.E. Observations of discrete, global magnetospheric oscillations directly driven by solar wind density variations. *J. Geophys. Res.: Space Phys.* 2003, vol. 108, 1257. DOI: [10.1029/2002JA009676](https://doi.org/10.1029/2002JA009676).
- Kepko L., Spence H.E., Singer H.J. ULF waves in the solar wind as direct drivers of magnetospheric pulsations. *Geophys. Res. Lett.* 2002, vol. 29, iss. 8, pp. 39-1–39-4. DOI: [10.1029/2001GL014405](https://doi.org/10.1029/2001GL014405).
- Khomenko E. Multi-Fluid Effects in Magnetohydrodynamics. *Oxford Research Encyclopedia of Physics*. 2022. DOI: [10.1093/acrefore/9780190871994.013.4](https://doi.org/10.1093/acrefore/9780190871994.013.4).
- Kleimenova N.G. Geomagnetic pulsations. *Model of Space*. Vol. 1. Eds. M.I. Panasyuk, L.S. Novikov. Moscow, KDU, 2007, pp. 611–626. (In Russian).
- Kleimenova N.G., Kozyreva O.V., Bitterli J. Longperiod geomagnetic pulsations in the theta aurora region on May 11, 1983. *Geomagnetism, Aeronomy*. 1995, vol. 35, pp. 44–48.
- Klimushkin D.Y. Resonators for hydromagnetic waves in the magnetosphere. *J. Geophys. Res.* 1998, vol. 103, iss. A2, pp. 2369–2375. DOI: [10.1029/97JA02193](https://doi.org/10.1029/97JA02193).
- Klimushkin D.Yu., Mager P.N. Spatial structure and stability of coupled Alfvén and drift compressional modes in non-uniform magnetosphere: Gyrokinetic treatment. *Planetary and Space Sci.* 2011, vol. 59, pp. 1613–1620. DOI: [10.1016/j.pss.2011.07.010](https://doi.org/10.1016/j.pss.2011.07.010).
- Klimushkin D.Yu., Mager P.N., Glassmeier K.-H. Toroidal and poloidal Alfvén waves with arbitrary azimuthal wave numbers in a finite pressure plasma in the Earth’s magnetosphere. *Ann. Geophys.* 2004, vol. 22, pp. 267–287. DOI: [10.5194/angeo-22-267-2004](https://doi.org/10.5194/angeo-22-267-2004).
- Klimushkin D.Yu., Mager P.N., Marilovtseva O.S. Parallel structure of Pc1 ULF oscillations in multi-ion magnetospheric plasma at finite ion gyrofrequency. *J. Atmos. Solar-Terr. Phys.* 2010, vol. 72, pp. 1327–1332. DOI: [10.1016/j.jastp.2010.09.019](https://doi.org/10.1016/j.jastp.2010.09.019).
- Klimushkin D.Yu., Mager P.N., Pilipenko V.A. On the ballooning instability of the coupled Alfvén and drift compressional modes. *Earth, Planets and Space*. 2012, vol. 64, pp. 777–781. DOI: [10.5047/eps.2012.04.002](https://doi.org/10.5047/eps.2012.04.002).
- Klimushkin D.Y., Nakariakov V.M., Mager P.N., Chermnykh O.K. Corrugation instability of a coronal arcade. *Solar Phys.* 2017, vol. 292, 184. DOI: [10.1007/s11207-017-1209-x](https://doi.org/10.1007/s11207-017-1209-x).
- Klimushkin D., Mager P., Chelpanov M., Kostarev D. Interaction between long-period ULF waves and charged particles in the magnetosphere: Theory and observations (Overview). *Solar-Terr. Phys.* 2021. vol. 7, iss. 4, pp. 33–66. DOI: [10.12737/stp-74202105](https://doi.org/10.12737/stp-74202105).
- Kobanov N.I., Chelpanov A.A. Oscillations accompanying HeI 10830 Å negative flare in a solar facula. II. Response of the transition region and corona. *Solar Phys.* 2019, vol. 294, iss. 5, p. A58. DOI: [10.1007/s11207-019-1449-z](https://doi.org/10.1007/s11207-019-1449-z).
- Kobanov N.I., Makarchik D.V. Developing modulationless measuring of magnetic fields and differential velocities at Sayan observatory. *Il Nuovo Cimento*. 2002, vol. 25, iss. 5-6, p. 695.
- Kobanov N.I., Chelpanov A.A., Kolobov D.Y. Oscillations above sunspots from the temperature minimum to the corona. *Astron. Astrophys.* 2013, vol. 554, A146. DOI: [10.1051/0004-6361/201220548](https://doi.org/10.1051/0004-6361/201220548).
- Korotova G., Sibeck D., Engebretson M., Wygant J., Thaller S., Spence H., et al. Multipoint spacecraft observations of long-lasting poloidal Pc4 pulsations in the dayside magnetosphere on 1–2 May 2014. *Ann. Geophys.* 2016, vol. 34, pp. 985–998. DOI: [10.5194/angeo-34-985-2016](https://doi.org/10.5194/angeo-34-985-2016).
- Korotova G., Sibeck D., Thaller S., Wygant J., Spence H., Kletzing C., et al. Multisatellite observations of the magnetosphere response to changes in the solar wind and interplanetary magnetic field. *Ann. Geophys.* 2018, vol. 36, pp. 1319–1333. DOI: [10.5194/angeo-36-1319-2018](https://doi.org/10.5194/angeo-36-1319-2018).
- Kostarev D.V., Mager P.N. Drift-compression waves propagating in the direction of energetic electron drift in the magnetosphere. *Solar-Terr. Phys.* 2017, vol. 3, iss. 3, pp. 20–29. DOI: [10.12737/stp-33201703](https://doi.org/10.12737/stp-33201703).
- Kostarev D.V., Mager P.N., Klimushkin D.Y. Alfvén wave parallel electric field in the dipole model of the magnetosphere: gyrokinetic treatment. *J. Geophys. Res.: Space Phys.* 2021, vol. 126, iss. 2. e2020JA028611. DOI: [10.1029/2020JA028611](https://doi.org/10.1029/2020JA028611).
- Kotova G.A., Leonovich A.S., Mazur V.A., Kovtyukh A.S., Panasyuk M.I., Trakhtengerts V.Yu., Demekhov A.G. Inner magnetosphere. *Plasma Heliogeophysics*. Eds. Zelenyi L.M., Veselovsky I.S. Moscow, Fizmatlit Publ., 2008, pp. 484–569. (In Russian).
- Kovadlo P.G., Lubkov A.A., Bevzov A.N., Budnikov K., Vlasov S.V., Zotov A.A., et al. Automation system for the Large Solar Vacuum Telescope. *Optoelectronics, Instrumentation and Data Processing*. 2016, vol. 52, pp. 187–195. DOI: [10.3103/S8756699016020126](https://doi.org/10.3103/S8756699016020126).
- Kovtyukh A.S. Geocorona of hot plasma. *Cosmic Res.* 2001, vol. 39, pp. 527–558. DOI: [10.1023/A:1013074126604](https://doi.org/10.1023/A:1013074126604).
- Krieger A.S., Timothy A.F., Roelof E.C. A coronal hole and its identification as the source of a high velocity solar wind stream. *Solar Phys.* 1973, vol. 29, iss 2, pp. 505–525. DOI: [10.1007/BF00150828](https://doi.org/10.1007/BF00150828).
- Landau L.D. On oscillations of electron plasma. *J. Experimental and Theoretical Phys.* 1946, vol. 16, p. 574. (In Russian).
- Le G., Chi P.J., Strangeway R.J., Russell C.T., Slavin J.A., Takahashi K., et al. Global observations of magnetospheric high- m poloidal waves during the 22 June 2015 magnetic storm. *Geophys. Res. Lett.* 2017, vol. 44, pp. 3456–3464. DOI: [10.1002/2017GL073048](https://doi.org/10.1002/2017GL073048).

- Lemen J.R., Title A.M., Akin D.J., Boerner P.F., Chou., Drake J.F., et al. The Atmospheric Imaging Assembly (AIA) on the Solar Dynamics Observatory (SDO). *Solar Phys.* 2012, vol. 275, iss. 1-2, pp. 17–40. DOI: [10.1007/s11207-011-9776-8](https://doi.org/10.1007/s11207-011-9776-8).
- Leonovich A.S., Mazur V.A. Resonance excitation of standing Alfvén waves in an axisymmetric magnetosphere (monochromatic oscillations). *Planetary and Space Sci.* 1989, vol. 37, iss. 9, pp. 1095–1108. DOI: [10.1016/0032-0633\(89\)90081-0](https://doi.org/10.1016/0032-0633(89)90081-0).
- Leonovich A.S., Mazur V.A. A theory of transverse small-scale standing Alfvén waves in an axially symmetric magnetosphere. *Planetary and Space Sci.* 1993, vol. 41, iss. 9, pp. 697–717. DOI: [10.1016/0032-0633\(93\)90055-7](https://doi.org/10.1016/0032-0633(93)90055-7).
- Leonovich A.S., Mazur V.A. On resonance properties of the Earth's magnetosphere. *International Conference "Solar-Terrestrial Relations and Physics of Earthquake Precursors"*. September 9–13, 2013, pp. 111–118. (In Russian).
- Leonovich A.S., Mazur V.A. *Linear theory of MHD oscillations of the magnetosphere*. Moscow, Fizmatlit Publ., 2016, 480 p. (In Russian).
- Leonovich A.S., Mishin V.V., Cao J.B. Penetration of magnetosonic waves into the magnetosphere: influence of a transition layer. *Ann. Geophys.* 2003, vol. 21, pp. 1083–1093. DOI: [10.5194/angeo-21-1083-2003](https://doi.org/10.5194/angeo-21-1083-2003).
- Leonovich A.S., Kozlov D.A., Pilipenko V.A. Magnetosonic resonance in a dipole-like magnetosphere. *Ann. Geophys.* 2006, vol. 24, pp. 2277–2289. DOI: [10.5194/angeo-24-2277-2006](https://doi.org/10.5194/angeo-24-2277-2006).
- Leonovich A.S., Klimushkin D.Y., Mager P.N. Experimental evidence for the existence of monochromatic transverse small-scale standing Alfvén waves with spatially dependent polarization. *J. Geophys. Res.: Space Phys.* 2015, vol. 120, iss. 7, pp. 5443–5454. DOI: [10.1002/2015JA021044](https://doi.org/10.1002/2015JA021044).
- Lifshits A.E., Fedorov E.N. Hydromagnetic oscillations of the magnetospheric-ionospheric resonator. *Proc. Academy of Sciences.* 1986, vol. 287, iss. 1, pp. 90–95. (In Russian).
- Mager P.N., Klimushkin D.Yu. Alfvén ship waves: high-m ULF pulsations in the magnetosphere generated by a moving plasma inhomogeneity. *Ann. Geophys.* 2008, vol. 26, iss. 6, pp. 1653–1663. DOI: [10.5194/angeo-26-1653-2008](https://doi.org/10.5194/angeo-26-1653-2008).
- Mager P.N., Klimushkin D.Y., Kostarev D.V. Drift-compressional modes generated by inverted plasma distributions in the magnetosphere. *J. Geophys. Res.: Space Phys.* 2013, vol. 118, pp. 4915–4923. DOI: [10.1002/jgra.50471](https://doi.org/10.1002/jgra.50471).
- Mager P.N., Mikhailova O.S., Mager O.V., Klimushkin D.Y. Eigenmodes of the transverse Alfvénic resonator at the plasma-pause: A Van Allen Probes case study. *Geophys. Res. Lett.* 2018, vol. 45, iss. 20, pp. 10796–0804. DOI: [10.1029/2018GL079596](https://doi.org/10.1029/2018GL079596).
- Mandal S., Yuan D., Fang X., Banerjee D., Pant V., van Doorselaere T. Reflection of propagating slow magneto-acoustic waves in hot coronal loops: Multi-instrument observations and numerical modeling. *Astrophys. J.* 2016, vol. 828, iss. 2, p. 72. DOI: [10.3847/0004-637X/828/2/72](https://doi.org/10.3847/0004-637X/828/2/72).
- Marcucci M.F., Bavassano Cattaneo M.B., Pallochia G., Amata E., Bruno R., Di Lellis A.M., et al. Energetic magnetospheric oxygen in the magnetosheath and its response to IMF orientation: Cluster observations. *J. Geophys. Res.: Space Phys.* 2004, vol. 109, iss. A7. A07203. DOI: [10.1029/2003JA010312](https://doi.org/10.1029/2003JA010312).
- Marsch E. Solar Wind and Kinetic Heliophysics - Hannes Alfvén Medal Lecture at the EGU General Assembly 2018. *Proc. 20th EGU General Assembly*. 4–13 April, 2018, Vienna, Austria, pp. 1790.
- Mauk B.H., Fox N.J., Kanekal S.G., Kessel R.L., Sibeck D.G., Ukhorskiy A. Science objectives and rationale for the Radiation Belt Storm Probes Mission. *Space Sci. Rev.* 2013, vol. 179, pp. 3–27. DOI: [10.1007/s11214-012-9908-y](https://doi.org/10.1007/s11214-012-9908-y).
- Mazur V.A. Resonance excitation of the magnetosphere by hydromagnetic waves incident from solar wind. *Plasma Phys. Rep.* 2010, vol. 36, iss. 11, pp. 953–963. DOI: [10.1134/S1063780X10110048](https://doi.org/10.1134/S1063780X10110048).
- Mazur V.A., Chuiko D.A. Energy flux in 2-D MHD waveguide in the outer magnetosphere. *J. Geophys. Res.: Space Phys.* 2017, vol. 122, pp. 1946–1959. DOI: [10.1002/2016JA023632](https://doi.org/10.1002/2016JA023632).
- McIntosh S.W., De Pontieu B., Carlsson M., Hansteen V., Boerner P., Goossens M. Alfvénic waves with sufficient energy to power the quiet solar corona and fast solar wind. *Nature.* 2011, vol. 475, pp. 477–480. DOI: [10.1038/nature10235](https://doi.org/10.1038/nature10235).
- McPherron R.L. Magnetic Pulsations: Their sources and relation to solar wind and geomagnetic activity. *Surveys in Geophys.* 2005, vol. 26, pp. 545–592. DOI: [10.1007/s10712-005-1758-7](https://doi.org/10.1007/s10712-005-1758-7).
- Mead G.D., Fairfield D.H. A quantitative magnetospheric model derived from spacecraft magnetometer data. *J. Geophys. Res.* 1975, vol. 80, iss. 4, pp. 523–534. DOI: [10.1029/JA080i004p00523](https://doi.org/10.1029/JA080i004p00523).
- Menk F.W. Magnetospheric ULF waves: A review. *The Dynamic Magnetosphere. IAGA Special Sopron Book Ser.* Eds. W. Liu. M. Fujimoto. 2011, vol. 3. Dordrecht: Springer Netherlands, 2011, pp. 223–256. DOI: [10.1007/978-94-007-0501-2_13](https://doi.org/10.1007/978-94-007-0501-2_13).
- Mikhailova O.S., Mager P.N., Klimushkin D.Y. Two modes of ion-ion hybrid waves in magnetospheric plasma. *Plasma Phys. and Controlled Fusion.* 2020a, vol. 62, iss. 2, 025026. DOI: [10.1088/1361-6587/ab5b32](https://doi.org/10.1088/1361-6587/ab5b32).
- Mikhailova O.S., Mager P.N., Klimushkin D.Y. Transverse resonator for ion-ion hybrid waves in dipole magnetospheric plasma. *Plasma Phys. and Controlled Fusion.* 2020b, vol. 62, iss. 9. 095008. DOI: [10.1088/1361-6587/ab9be9](https://doi.org/10.1088/1361-6587/ab9be9).
- Mikhailova O.S., Klimushkin D.Yu., Mager P.N. The current state of the theory of Pc1 range ULF pulsations in magnetospheric plasma with heavy ions: A review. *Solar-Terr. Phys.* 2022a. Vol. 8. Iss. 1. P. 3–18. DOI: [10.12737/stp-81202201](https://doi.org/10.12737/stp-81202201).
- Mikhailova O.S., Smotrova E.E., Mager P.N. Resonant generation of an Alfvén wave by a substorm injected electron cloud: A Van Allen probe case study. *Geophys. Res. Lett.* 2022b. Vol. 49, no. 19. e2022GL100433. DOI: [10.1029/2022GL100433](https://doi.org/10.1029/2022GL100433).
- Mikhailovskii A.B., Fridman A.M. Drift waves in a finite-pressure plasma. *Soviet Physics-JETP.* 1967, vol. 24, iss. 5, pp. 965–974.
- Miyoshi Y., Shinohara I., Takashima T., Asamura K., Higashio N., Mitani T., et al. Geospace exploration project ERG. *Earth, Planets and Space.* 2018, vol. 70. 101. DOI: [10.1186/s40623-018-0862-0](https://doi.org/10.1186/s40623-018-0862-0).
- Morton R.J., Tomczyk S., Pinto R. Investigating Alfvénic wave propagation in coronal open-field regions. *Nature Communications.* 2015, vol. 6, p. 7813. DOI: [10.1038/ncomms8813](https://doi.org/10.1038/ncomms8813).
- Motoba T., Ogawa Y., Ebihara Y., Kadokura A., Gerard A.J., Weatherwax A.T. Daytime Pc5 diffuse auroral pulsations and their association with outer magnetospheric ULF waves. *J. Geophys. Res.: Space Phys.* 2021, vol. 126, iss. 8. e2021JA029218. DOI: [10.1029/2021JA029218](https://doi.org/10.1029/2021JA029218).
- Nakariakov V.M., Verwichte E. Coronal waves and oscillations. *Living Reviews in Solar Physics.* 2005, vol. 2, iss. 3. DOI: [10.12942/lrsp-2005-3](https://doi.org/10.12942/lrsp-2005-3).
- Nakariakov V.M., Melnikov V.F., Reznikova V.E. Global sausage modes of coronal loops. *Astron. Astrophys.* 2003, vol. 412, pp. L7–L10. DOI: [10.1051/0004-6361:20031660](https://doi.org/10.1051/0004-6361:20031660).
- Nakariakov V.M., Pascoe D.J., Arber T.D. Short quasi-periodic MHD waves in coronal structures. *Space Sci. Rev.* 2005, vol. 121, iss. 1-4, pp. 115–125. DOI: [10.1007/s11214-006-4718-8](https://doi.org/10.1007/s11214-006-4718-8).

- Nakariakov V.M., Anfinogentov S.A., Nisticò G., Lee D.-H. Undamped transverse oscillations of coronal loops as a self-oscillatory process. *Astron. Astrophys.* 2016a, vol. 591, L5. DOI: [10.1051/0004-6361/201628850](https://doi.org/10.1051/0004-6361/201628850).
- Nakariakov V.M., Pilipenko V., Heilig B., Jelínek P., Karlický M., Klimushkin D.Y., et al. Magneto-hydrodynamic oscillations in the solar corona and Earth's magnetosphere: Towards consolidated understanding. *Space Sci. Rev.* 2016b, vol. 200, pp. 75–203. DOI: [10.1007/s11214-015-0233-0](https://doi.org/10.1007/s11214-015-0233-0).
- Nakariakov V.M., Anfinogentov S.A., Antolin P., Jain R., Kolotkov D.Y., Kupriyanova E.G., et al. Oscillations of coronal loops. *Space Sci. Rev.* 2021, vol. 217, iss. 6, article id. 73. DOI: [10.1007/s11214-021-00847-2](https://doi.org/10.1007/s11214-021-00847-2).
- Nielsen E. The STARE system and some of its applications. *The IMS Source Book: Guide to the International Magnetospheric Study Data Analysis*. Eds. C.T. Russel, D.J. Southwood. Washington DC: AGU, 1982, pp. 213–224.
- Nishitani N., Ruohoniemi J.M., Lester M., Baker J.B.H., Koustov A.V., Shepherd S.G., et al. Review of the accomplishments of mid-latitude Super Dual Auroral Radar Network (SuperDARN) HF radars. *Progress in Earth and Planetary Sci.* 2019, vol. 6, iss. 1, p. 27. DOI: [10.1186/s40645-019-0270-5](https://doi.org/10.1186/s40645-019-0270-5).
- Ofman L., Wang T. hot coronal loop oscillations observed by SUMER: Slow magnetosonic wave damping by thermal conduction. *Astrophys. J.* 2002, vol. 580, iss. 1, pp. L85–L88. DOI: [10.1086/345548](https://doi.org/10.1086/345548).
- Oimatsu S., Nosé M., Takahashi K., Yamamoto K., Keika K., Kletzing C.A., et al. Van Allen Probes observations of drift-bounce resonance and energy transfer between energetic ring current protons and poloidal Pc4 wave. *J. Geophys. Res.: Space Phys.* 2018a, vol. 123, iss. 5, pp. 3421–3435. DOI: [10.1029/2017JA025087](https://doi.org/10.1029/2017JA025087).
- Oimatsu S., Nosé M., Teramoto M., Yamamoto K., Matsuo A., Kasahara S., et al. Drift-bounce resonance between Pc5 pulsations and ions at multiple energies in the nightside magnetosphere: Arase and MMS observations. *Geophys. Res. Lett.* 2018b, vol. 45, iss. 15, pp. 7277–7286. DOI: [10.1029/2018GL078961](https://doi.org/10.1029/2018GL078961).
- Papamastorakis I., Paschmann G., Sckopke N., Bame S.J., Berchem J. The magnetopause as a tangential discontinuity for large field rotation angles. *J. Geophys. Res.* 1984, vol. 89, iss. A1, pp. 127–135. DOI: [10.1029/JA089iA01p00127](https://doi.org/10.1029/JA089iA01p00127).
- Parker E.N. Interaction of the solar wind with the geomagnetic field. *Physics of Fluids*. 1958, vol. 1, pp. 171–187. DOI: [10.1063/1.1724339](https://doi.org/10.1063/1.1724339).
- Pilipenko V.A. ULF waves on the ground and in space. *J. Atmos. Terr. Phys.* 1990, vol. 52, no. 12, pp. 1193–1209. DOI: [10.1016/0021-9169\(90\)90087-4](https://doi.org/10.1016/0021-9169(90)90087-4).
- Pilipenko V., Belakhovsky V., Murr D., Fedorov E., Engebretson M. Modulation of total electron content by ULF Pc5 waves. *J. Geophys. Res.: Space Phys.* 2014, vol. 119, iss. 6, pp. 4358–4369. DOI: [10.1002/2013JA019594](https://doi.org/10.1002/2013JA019594).
- Plowman J., Kankelborg C., Martens P. Fast differential emission measure inversion of solar coronal data. *Astrophys. J.* 2013, vol. 771, no. 1, p. 2. DOI: [10.1088/0004-637X/771/1/2](https://doi.org/10.1088/0004-637X/771/1/2).
- Pokhotelov O.A., Pilipenko V.A., Amata E. Drift anisotropy instability of a finite- β magnetospheric plasma. *Planetary and Space Sci.* 1985, vol. 33, iss. 11, pp. 1229–1241. DOI: [10.1016/0032-0633\(85\)90001-7](https://doi.org/10.1016/0032-0633(85)90001-7).
- Ponomarenko P.P., Menk F.W., Waters C.L. Visualization of ULF waves in SuperDARN data. *Geophys. Res. Lett.* 2003, vol. 30, iss. 18, 1926. DOI: [10.1029/2003GL017757](https://doi.org/10.1029/2003GL017757).
- Potapov A.S., Mazur V.A. Pc3 pulsations: From the source in the upstream region to Alfvén resonances in the magnetosphere. Theory and observations. *Solar wind sources of magnetospheric ultralow frequency waves. Geophys. Monograph Ser.* 1994, vol. 81, Eds. M.J. Engebretson, K. Takahashi, M. Scholer. Washington DC: AGU, 1994, pp. 135–145. DOI: [10.1029/GM081p0135](https://doi.org/10.1029/GM081p0135).
- Potapov A.S., Polyushkina T.N. Experimental evidence for direct penetration of ULF waves from the solar wind and their possible effect on acceleration of radiation belt electrons. *Geomagnetism and Aeronomy.* 2010, vol. 50, no. 8, pp. 950–957. DOI: [10.1134/S0016793210080049](https://doi.org/10.1134/S0016793210080049).
- Potapov A.S., Polyushkina T.N., Pulyaev V.A. Observations of ULF waves in the solar corona and in the solar wind at the Earth's orbit. *J. Atmos. Solar-Terr. Phys.* 2013, vol. 102, pp. 235–242. DOI: [10.1016/j.jastp.2013.06.001](https://doi.org/10.1016/j.jastp.2013.06.001).
- Rakhmanova L., Riazantseva M., Zastenker G. Plasma and magnetic field turbulence in the Earth's magnetosheath at ion scales. *Frontiers in Astronomy and Space Sci.* 2021, vol. 7. DOI: [10.3389/fspas.2020.616635](https://doi.org/10.3389/fspas.2020.616635).
- Ren J., Zong Q. G., Miyoshi Y., Rankin R., Spence H.E., Funsten H.O., Wygant J.R., Kletzing C.A. A Comparative Study of ULF Waves' Role in the Dynamics of Charged Particles in the Plasmasphere: Van Allen Probes Observation. *J. Geophys. Res.: Space Phys.* 2018, Vol. 123, no. 7. P. 5334–5343. DOI: [10.1029/2018JA025255](https://doi.org/10.1029/2018JA025255).
- Ren J., Zong Q.-G., Zhou X.Z., Spence H.E., Funsten H.O., Wygant J.R., Rankin R. Cold Plasmaspheric Electrons Affected by ULF Waves in the Inner Magnetosphere: A Van Allen Probes Statistical Study. *J. Geophys. Res.: Space Phys.* 2019, Vol. 124, no. 10. P. 7954–7965. DOI: [10.1029/2019JA027009](https://doi.org/10.1029/2019JA027009).
- Reznikova V.E., van Doorselaere T., Kuznetsov A.A. Perturbations of gyrosynchrotron emission polarization from solar flares by sausage modes: forward modeling. *Astron. Astrophys.* 2015, vol. 575, A47. DOI: [10.1051/0004-6361/201424548](https://doi.org/10.1051/0004-6361/201424548).
- Rimmele T.R., Warner M., Keil S.L., Goode P.R., Knölker M., Kuhn J.R., et al. The Daniel K. Inouye Solar Telescope – Observatory Overview. *Solar Phys.* 2020, vol. 295, iss. 12. A172. DOI: [10.1007/s11207-020-01736-7](https://doi.org/10.1007/s11207-020-01736-7).
- Rincon F., Rieutord M. The Sun's supergranulation. *Living Reviews in Solar Physics.* 2018, vol. 15, 6. DOI: [10.1007/s41116-018-0013-5](https://doi.org/10.1007/s41116-018-0013-5).
- Robustini C., Esteban Pozuelo S., Leenaerts J., de la Cruz Rodríguez J. Chromospheric observations and magnetic configuration of a supergranular structure. *Astron. Astrophys.* 2019, vol. 621, p. A1. DOI: [10.1051/0004-6361/201833246](https://doi.org/10.1051/0004-6361/201833246).
- Rubtsov A.V., Mager P.N., Klimushkin D.Y. Ballooning instability of azimuthally small scale coupled Alfvén and slow magnetoacoustic modes in two-dimensionally inhomogeneous magnetospheric plasma. *Physics of Plasmas.* 2018a, vol. 25, iss. 10. 102903. DOI: [10.1063/1.5051474](https://doi.org/10.1063/1.5051474).
- Rubtsov A.V., Agapitov O.V., Mager P.N., Klimushkin D.Yu., Mager O.V., Mozer F.S., Angelopoulos V. Drift resonance of compressional ULF waves and substorm-injected protons from multipoint THEMIS measurements. *J. Geophys. Res.: Space Phys.* 2018b, vol. 123, iss. 11, pp. 9406–9419. DOI: [10.1029/2018JA025985](https://doi.org/10.1029/2018JA025985).
- Rubtsov A.V., Mager P.N., Klimushkin D.Y. Ballooning Instability in the Magnetospheric Plasma: Two-Dimensional Eigenmode Analysis. *J. Geophys. Res.: Space Phys.* 2020, vol. 125, iss. 1. e2019JA027024. DOI: [10.1029/2019JA027024](https://doi.org/10.1029/2019JA027024).
- Rubtsov A.V., Mikhailova O.S., Mager P.N., Klimushkin D.Y. Multi-spacecraft observation of the pre-substorm long-lasting poloidal ULF wave. *Geophys. Res. Lett.* 2021, vol. 48, iss. 23. e2021GL096182. DOI: [10.1029/2021GL096182](https://doi.org/10.1029/2021GL096182).
- Ruderman M.S., Roberts B. The Damping of Coronal Loop Oscillations. *Astrophys. J.* 2002, vol. 577, iss. 1, pp. 475–486. DOI: [10.1086/342130](https://doi.org/10.1086/342130).
- Samsonov A.A., Němeček Z., Šafránková J., Jelínek K. Why does the total pressure on the subsolar magnetopause differ from the solar wind dynamic pressure? *Cosmic Res.* 2013, vol. 51, iss. 1, pp. 37–45. DOI: [10.1134/S0010952513010073](https://doi.org/10.1134/S0010952513010073).

- Shi X., Baker J.B.H., Ruohoniemi J.M., Hartinger M.D., Murphy K.R., Rodriguez J.V., et al. Long-Lasting Poloidal ULF Waves Observed by Multiple Satellites and High-Latitude SuperDARN Radars. *J. Geophys. Res.: Space Phys.* 2018, vol. 123, iss. 10, pp. 8422–8438. DOI: [10.1029/2018JA026003](https://doi.org/10.1029/2018JA026003).
- Shukhobodskaya D., Shukhobodskiy A.A., Erdélyi R. Flute oscillations of cooling coronal loops with variable cross-section *Astron. Astrophys.* 2021, vol. 649, id. A36, 9 p. DOI: [10.1051/0004-6361/202140314](https://doi.org/10.1051/0004-6361/202140314).
- Snodgrass H.B., Wilson P.R. Real and Virtual Unipolar Regions. *Solar Phys.* 1993, vol. 148, iss. 2. P. 179–194. DOI: [10.1007/BF00645084](https://doi.org/10.1007/BF00645084).
- Soler R. Fluting modes in transversely nonuniform solar flux tubes. *Astrophys. J.* 2017, vol. 850, iss. 2, article id. 114, 10 p. DOI: [10.3847/1538-4357/aa956e](https://doi.org/10.3847/1538-4357/aa956e).
- Song W.-B., Feng X.-S., Shen F. The heating of the solar transition region. *Res. Astron. Astrophys.* 2010, vol. 10, iss. 6, pp. 529–532. DOI: [10.1088/1674-4527/10/6/002](https://doi.org/10.1088/1674-4527/10/6/002).
- Soto-Chavez A.R., Lanzerotti L.J., Manweiler J.W., Gerrard A., Cohen R., Xia Z., et al. Observational evidence of the drift-mirror plasma instability in Earth's inner magnetosphere. *Physics of Plasmas*. 2019, vol. 26, iss. 4. 042110. DOI: [10.1063/1.5083629](https://doi.org/10.1063/1.5083629).
- Southwood D.J. Some features of field line resonances in the magnetosphere. *Planetary and Space Sci.* 1974, vol. 22, iss. 3, pp. 483–491. DOI: [10.1016/0032-0633\(74\)90078-6](https://doi.org/10.1016/0032-0633(74)90078-6).
- Srivastava A., Shetye J., Murawski K., Doyle J., Stangalini M., Scullion E., Ray T., Wójcik D., Dwivedi B. High-frequency torsional Alfvén waves as an energy source for coronal heating. *Scientific Rep.* 2017, vol. 7, article id. 43147. DOI: [10.1038/srep43147](https://doi.org/10.1038/srep43147).
- Stephenson J.A.E., Walker A.D.M. HF radar observations of Pc5 ULF pulsations driven by the solar wind. *Geophys. Res. Lett.* 2002, vol. 29, iss. 9, pp. 8–1–8–4. DOI: [10.1029/2001GL014291](https://doi.org/10.1029/2001GL014291).
- Sterling A.C. Solar Spicules: A review of recent models and targets for future observations. *Solar Phys.* 2000, vol. 196, iss. 1, pp. 79–111. DOI: [10.1023/A:1005213923962](https://doi.org/10.1023/A:1005213923962).
- Takahashi K., Crabtree C., Ukhorskiy A.Y., Boyd A., Denton R.E., Turner D., et al. Van Allen Probes Observations of symmetric stormtime compressional ULF waves. *J. Geophys. Res.: Space Phys.* 2022, vol. 127. e2021JA030115. DOI: [10.1029/2021JA030115](https://doi.org/10.1029/2021JA030115).
- Thurgood J.O., Morton R.J., McLaughlin J.A. First direct measurements of transverse waves in solar polar plumes using SDO/AIA. *Astrophys. J. Lett.* 2014, vol. 790, iss. 1. L2. DOI: [10.1088/2041-8205/790/1/L2](https://doi.org/10.1088/2041-8205/790/1/L2).
- Trifonov V.D., Golovko A.A., Skomorovskiy V.I. Observations of the chromosphere in Baikal Astrophysical Observatory using CCD cameras. *Proc. National Conference devoted to 90th Anniversary of V.E. Stepanov, Corresponding Member of RAS.* 2004, pp. 178–180. (In Russian).
- Troitskaya V.A., Guglielmi A.V. Geomagnetic pulsations and diagnostics of the magnetosphere. *Soviet Physics Uspekhi.* 1969, vol. 12, iss. 2, pp. 195–218. DOI: [10.1070/PU1969v012n02ABEH003933](https://doi.org/10.1070/PU1969v012n02ABEH003933).
- Troitskaya V.A., Plyasova-Bakunina T.A., Gul'elmi A.V. The connection of Pc2-4 pulsations with the interplanetary magnetic field. *Proc. Academy of Sciences. Math. Phys.* 1971, vol. 197, iss. 6, pp. 1312–1314. (In Russian).
- Uchida Y., Altschuler M.D., Newkirk Jr.G. Flare-produced coronal MHD-fast-mode wavefronts and Moreton's wave phenomenon. *Solar Phys.* 1973, vol. 28, iss. 2, pp. 495–516. DOI: [10.1007/BF00152320](https://doi.org/10.1007/BF00152320).
- Vaisberg O.L., Smirnov V.N. Near-Earth shock wave. *Plasma Heliogeophysics.* Eds. Zelenyi L.M., Veselovsky I.S. Moscow, Fizmatlit Publ., 2008, pp. 378–422. (In Russian).
- van Doorselaere T., Brady C.S., Verwichte E., Nakariakov V.M. Seismological demonstration of perpendicular density structuring in the solar corona. *Astron. Astrophys.* 2008, vol. 491, iss. 2, pp. L9–L12. DOI: [10.1051/0004-6361:200810659](https://doi.org/10.1051/0004-6361:200810659).
- van Doorselaere T., Verwichte E., Terradas J. The Effect of Loop Curvature on Coronal Loop Kink Oscillations. *Space Sci. Rev.* 2009. Vol. 149. P. 299–324. DOI: [10.1007/s11214-009-9530-9](https://doi.org/10.1007/s11214-009-9530-9).
- Vetoulis G., Chen L. Global structures of Alfvén-ballooning modes in magnetospheric plasmas. *Geophys. Res. Lett.* 1994, vol. 21, pp. 2091–2094. DOI: [10.1029/94GL01703](https://doi.org/10.1029/94GL01703).
- Volkov T.F. Hydrodynamic description of highly rarefied plasma. *Plasma Phys.* Eds. Leontovich M.A. 1964, vol. 4, pp. 3–19. Moscow, Gosatomizdat Publ., 1964. (In Russian).
- Walker A.D.M., Greenwald R.A. Pulsation structure in the ionosphere derived from aurora radar data. *ULF Pulsations in the Magnetosphere.* Ed. D.J. Southwood. Dordrecht: Springer, 1981, pp. 111–127. DOI: [10.1007/978-94-009-8426-4_7](https://doi.org/10.1007/978-94-009-8426-4_7).
- Walker A.D.M., Greenwald R.A., Stuart W.F., Green C.A. Stare auroral radar observations of Pc 5 geomagnetic pulsations. *J. Geophys. Res.* 1979, vol. 84, iss. A7, pp. 3373–3388. DOI: [10.1029/JA084iA07p03373](https://doi.org/10.1029/JA084iA07p03373).
- Wang Y.-M. EIT Waves and fast-mode propagation in the solar corona. *Astrophys. J.* 2000, vol. 543, iss. 1, p. L89. DOI: [10.1086/318178](https://doi.org/10.1086/318178).
- Wang Y.-M. Coronal Holes and Open Magnetic Flux. *Space Sci. Rev.* 2009, vol. 144, pp. 383–399. DOI: [10.1007/s11214-008-9434-0](https://doi.org/10.1007/s11214-008-9434-0).
- Wang T.J., Solanki S.K., Curdt W., Innes D.E., Dammasch I.E., Kliem B. Hot coronal loop oscillations observed with SUMER: Examples and statistics. *Astron. Astrophys.* 2003, vol. 406, iss. 3, pp. 1105–1121. DOI: [10.1051/0004-6361:20030858](https://doi.org/10.1051/0004-6361:20030858).
- Weberg M.J., Morton R.J., McLaughlin J.A. An automated algorithm for identifying and tracking transverse waves in solar images. *Astrophys. J.* 2018, vol. 852, iss. 1, p. 57. DOI: [10.3847/1538-4357/aa9e4a](https://doi.org/10.3847/1538-4357/aa9e4a).
- Welling D.T., André M., Dandouras I., Delcourt D., Fazakerley A., Fontaine D., et al. The Earth: Plasma sources, losses, and transport processes. *Space Sci. Rev.* 2015, vol. 192, pp. 145–208. DOI: [10.1007/s11214-015-0187-2](https://doi.org/10.1007/s11214-015-0187-2).
- Wiegmann T., Solanki S.K., Borrero J.M., Martínez Pilet V., del Toro Iniesta J.C., Domingo V., et al. Magnetic loops in the quiet Sun. *Astrophys. J. Lett.* 2010, vol. 723, pp. L185–L189. DOI: [10.1088/2041-8205/723/2/L185](https://doi.org/10.1088/2041-8205/723/2/L185).
- Yagova N., Heilig B., Fedorov E. Pc2-3 geomagnetic pulsations on the ground, in the ionosphere, and in the magnetosphere: MM100, CHAMP, and THEMIS observations. *Ann. Geophys.* 2015, vol. 33, iss. 1, pp. 117–128. DOI: [10.5194/angeo-33-117-2015](https://doi.org/10.5194/angeo-33-117-2015).
- Yamamoto T., Hayashi K., Kokubun S., Oguti T., Ogawa T. Auroral activities and long-period geomagnetic pulsations. I. Pc5 pulsations and concurrent auroras in the dawn sector. II. Ps5 pulsations following auroral breakup in the premidnight hours. *J. Geomagnetism and Geoelectricity*, 1988, vol. 40, iss. 5, pp. 553–569. DOI: [10.5636/jgg.40.553](https://doi.org/10.5636/jgg.40.553).
- Yan Y., Chen Z., Wang W., Liu F., Geng L., Chen L., et al. Mingantu Spectral Radioheliograph for solar and space weather studies. *Frontiers in Astron. and Space Sci.* 2021, vol. 8, p. 20. DOI: [10.3389/fspas.2021.584043](https://doi.org/10.3389/fspas.2021.584043).
- Yeoman T.K., James M., Mager P.N., Klimushkin D.Y. SuperDARN observations of high-m ULF waves with curved phase fronts and their interpretation in terms of transverse resonator theory. *J. Geophys. Res.: Space Phys.* 2012, vol. 117, iss. A6. A06231. DOI: [10.1029/2012JA017668](https://doi.org/10.1029/2012JA017668).

Yumoto K. Characteristics of localized resonance coupling oscillations of the slow magnetosonic wave in a non-uniform plasma. *Planetary Space Sci.* 1985, vol. 33. pp. 1029–1036.

Zaitsev V.V., Stepanov A.V. On the origin of pulsations of type IV solar radio emission. Plasma cylinder oscillations (I). *Research on Geomagnetism, Aeronomy and Solar Physics.* 1975, iss. 37, pp. 3–10. (In Russian).

Zayer I., Solanki S.K., Stenflo J.O. The internal magnetic distribution and the diameters of solar magnetic elements. *Astron. Astrophys.* 1989, vol. 211, pp. 463–475.

Zelenyi L.M., Veselovsky I.S. *Plasma Heliogeophysics.* Moscow, Fizmatlit Publ., 2008. 672 p. (In Russian).

Zhang H., Ai G., Sakurai T., Kurokawa H. Fine structures of chromospheric magnetic field and material flow in a solar active region. *Solar Phys.* 1991, vol. 136, iss. 2, pp. 269–293. DOI: [10.1007/BF00146536](https://doi.org/10.1007/BF00146536).

Zheleznyakov V.V., Zlotnik E.Y. Thermal cyclotron radiation from solar active regions. *Intern. Symposium Astron. Union.* 1980, vol. 86, pp. 87–99.

Zong Q. Magnetospheric response to solar wind forcing: ULF wave — particle interaction perspective. *Ann. Geophys.* 2022, vol. 40, iss.1, pp. 121–150, DOI: [10.5194/angeo-40-121-2022](https://doi.org/10.5194/angeo-40-121-2022).

Zong Q.-G., Zhou X.-Z., Wang Y.F., Li X., Song P., Baker D.N., et al. Energetic electron response to ULF waves induced by interplanetary shocks in the outer radiation belt. *J. Geophys. Res.* 2009, vol. 114, A10204. DOI: [10.1029/2009JA014393](https://doi.org/10.1029/2009JA014393).

Zong Q.-G., Rankin R., Zhou X. The interaction of ultra-low-frequency pc3-5 waves with charged particles in Earth's magnetosphere. *Rev. Modern Plasma Phys.* 2017, vol. 1, p. 10. DOI: [10.1007/s41614-017-0011-4](https://doi.org/10.1007/s41614-017-0011-4).

URL: <https://www.nasa.gov/feature/goddard/2021/nasa-enters-the-solar-atmosphere-for-the-first-time-bringing-new-discoveries> (accessed February 8, 2022).

URL: <http://ckp-rf.ru/ckp/3056> (accessed February 8, 2022).

Original Russian version: Chelpanov M.A., Anfinogentov S.A., Kostarev D.V., Mikhailova O.S., Rubtsov A.V., Fedenev V.V., Chelpanov A.A., published in *Solnechno-zemnaya fizika.* 2022. Vol. 8. Iss. 4. P. 3–28. DOI: [10.12737/szf-84202201](https://doi.org/10.12737/szf-84202201). © 2022 INFRA-M Academic Publishing House (Nauchno-Izdatelskii Tsentr INFRA-M).

How to cite this article

Chelpanov M.A., Anfinogentov S.A., Kostarev D.V., Mikhailova O.S., Rubtsov A.V., Fedenev V.V., Chelpanov A.A. Review and comparison of MHD wave characteristics at the Sun and in Earth's magnetosphere. *Solar-Terrestrial Physics.* 2022. Vol. 8. Iss. 4. P. 3–27. DOI: [10.12737/stp-84202201](https://doi.org/10.12737/stp-84202201).